




TCF1-positive and TCF1-negative TRM CD8 T cell subsets and cDC1s orchestrate melanoma protection and immunotherapy response

Saraí G De León-Rodríguez ^{1,2}, Cristina Aguilar-Flores,³ Julián A Gajón,^{2,4} Ángel Juárez-Flores,^{2,5} Alejandra Mantilla,⁶ Raquel Gerson-Cwilich,⁷ José Fabián Martínez-Herrera,^{7,8} Diana Alejandra Villegas-Osorno,⁷ Claudia T Gutiérrez-Quiroz,⁹ Sergio Buenaventura-Cisneros,¹⁰ Mario Alberto Sánchez-Prieto,^{10,11} Edmundo Castelán-Maldonado,¹⁰ Samuel Rivera Rivera,^{7,11} Ezequiel M Fuentes-Panana ⁵, Laura C Bonifaz ^{2,12}

To cite: De León-Rodríguez SG, Aguilar-Flores C, Gajón JA, *et al.* TCF1-positive and TCF1-negative TRM CD8 T cell subsets and cDC1s orchestrate melanoma protection and immunotherapy response. *Journal for ImmunoTherapy of Cancer* 2024;**12**:e008739. doi:10.1136/jitc-2023-008739

► Additional supplemental material is published online only. To view, please visit the journal online (<https://doi.org/10.1136/jitc-2023-008739>).

Accepted 10 June 2024



© Author(s) (or their employer(s)) 2024. Re-use permitted under CC BY-NC. No commercial re-use. See rights and permissions. Published by BMJ.

For numbered affiliations see end of article.

Correspondence to

Dr Ezequiel M Fuentes-Panana; empanana@yahoo.com

Dr Laura C Bonifaz; lbonifaz@yahoo.com

ABSTRACT

Background Melanoma, the most lethal form of skin cancer, has undergone a transformative treatment shift with the advent of checkpoint blockade immunotherapy (CBI). Understanding the intricate network of immune cells infiltrating the tumor and orchestrating the control of melanoma cells and the response to CBI is currently of utmost importance. There is evidence underscoring the significance of tissue-resident memory (TRM) CD8 T cells and classic dendritic cell type 1 (cDC1) in cancer protection. Transcriptomic studies also support the existence of a *TCF7+* (encoding TCF1) T cell as the most important for immunotherapy response, although uncertainty exists about whether there is a TCF1+TRM T cell due to evidence indicating TCF1 downregulation for tissue residency activation.

Methods We used multiplexed immunofluorescence and spectral flow cytometry to evaluate TRM CD8 T cells and cDC1 in two melanoma patient cohorts: one immunotherapy-naïve and the other receiving immunotherapy. The first cohort was divided between patients free of disease or with metastasis 2 years postdiagnosis while the second between CBI responders and non-responders.

Results Our study identifies two CD8+TRM subsets, TCF1+ and TCF1-, correlating with melanoma protection. TCF1+TRM cells show heightened expression of IFN- γ and Ki67 while TCF1- TRM cells exhibit increased expression of cytotoxic molecules. In metastatic patients, TRM subsets undergo a shift in marker expression, with the TCF1- subset displaying increased expression of exhaustion markers. We observed a close spatial correlation between cDC1s and TRMs, with TCF1+TRM/cDC1 pairs enriched in the stroma and TCF1- TRM/cDC1 pairs in tumor areas. Notably, these TCF1- TRMs express cytotoxic molecules and are associated with apoptotic melanoma cells. Both TCF1+ and TCF1- TRM subsets, alongside cDC1, prove relevant to CBI response.

Conclusions Our study supports the importance of TRM CD8 T cells and cDC1 in melanoma protection while also highlighting the existence of functionally distinctive TCF1+

WHAT IS ALREADY KNOWN ON THIS TOPIC

⇒ With the recent integration of immunotherapy into cancer treatment, there is an intensified effort to identify responsive immune populations for enhanced treatment outcomes. Three key immune populations—TCF1+ memory T cells, tissue-resident memory (TRM) CD8 T cells, and cDC1s—have emerged as pivotal components in anticancer immunity. Experimental models of chronic infection and cancer also emphasize TCF1+ memory T cells as primary responders to checkpoint immunotherapy. However, transcriptional studies support mutual exclusion between TCF1 expression and the TRM program.

and TCF1- TRM subsets, both crucial for melanoma control and CBI response.

BACKGROUND

Immunotherapy has emerged as a groundbreaking approach in cancer treatment, notably exemplified in the context of melanoma. Checkpoint blockade immunotherapy (CBI) disrupts inhibitory signals exploited by tumors to evade immune detection, harnessing the immune system to eliminate cancer cells. This results in enduring responses and extended survival for a significant fraction of melanoma patients.¹ As CBI gains recognition as a primary therapy for unresectable or metastatic melanoma, understanding the intricate landscape of tumor-infiltrating immune cells becomes imperative for tailoring effective treatment strategies.

Transcriptomic studies have revealed several subsets of tumor-infiltrating CD8 T cells (CD8 TIL), most of which express PD1,

WHAT THIS STUDY ADDS

⇒ We validated the existence of TCF1+TRM CD8 T cells, which concurrently with TCF1 express CD103, CD69, CD45RO, Hobit, and RunX3, markers of an active TRM program. TCF1+TRM appeared to shift from a progenitor-like stage, marked by heightened IFN- γ and Ki67 expression, to a TCF1- stage characterized by increased cytolytic protein expression. In patients losing control over melanoma progression, the TCF1- TRM subset undergoes a further shift, accumulating checkpoint inhibitors. We observed a close spatial correlation between cDC1s and both TRM subsets, with cytotoxic TCF1- TRM enriched in tumor areas and associating with apoptotic tumor cells. In addition to describe the importance of the TCF1+ and TCF1- CD8 TRM, our study is the first to document the association of cDC1 with immunotherapy response in clinical settings.

HOW THIS STUDY MIGHT AFFECT RESEARCH, PRACTICE OR POLICY

⇒ Our study highlights the significance of three distinct immune cell populations in melanoma control and response to immunotherapy: TCF1+ and TCF1- CD8 TRMs, and cDC1 dendritic cells. Furthermore, we demonstrate the effectiveness of a seven-marker staining panel (TCF1, CD103, CD8, BDCA3, CD11c, HLA-DR, and nuclei) for identifying these cells within the tumor stroma. This approach can help identify patients at higher risk of poor outcomes and those likely to benefit from immunotherapy. Importantly, our staining protocol is easily adaptable for use in hospital settings, including those in developing countries.

categorizing them as exhausted.² Despite the expression of exhaustion markers, these PD1+ CD8 TILs remain functional and efficient in controlling cancer cells and chronic infections.³ A distinctive differentiation pathway has been observed, going from progenitor cells to cells with enhanced cytotoxicity, ultimately leading to dysfunctional cells unable to control tumor growth.^{4,5} Notably, the transcription factor T cell factor 7 (*TCF7* encodes for TCF1) is expressed at progenitor stages, and is the population giving rise to CD8 T cells with enhanced cytotoxic activity, which eventually become terminally exhausted after accumulating expression of several checkpoint inhibitors and displaying evidence of altered metabolism with mitochondrial dysfunction.⁴⁻⁷

Tissue-resident memory (TRM) CD8 T cells are normal inhabitants of peripheral tissues, including tumor sites. Numerous studies highlight their strategic location, enabling rapid and targeted responses to pathogens and cancer cells, contributing to site-specific immunosurveillance. TRM CD8 T cells exhibit superior cytotoxic and cytokine expression activity compared with non-TRM CD8 T cells,⁸⁻¹⁰ making them a key immune cell in cancer control, as it has been demonstrated in both experimental murine melanoma models and clinical studies.¹¹⁻¹³ TRM T cells residing in tumors often express a variety of checkpoint inhibitors while still exhibiting evidence of effector activity.^{8,9,14,15} Since immunotherapy relies on the expression of checkpoint inhibitors, TRM CD8 T cells emerge as a key population for fostering and recovering their effector activity, making them crucial for the success of

immunotherapeutic interventions. Indeed, recent investigations underscore the importance of TRM T cells in achieving CBI-positive responses.^{12,16}

It is currently uncertain whether tumor-infiltrating TRM T cells can be separated into progenitor, effector and terminally exhausted subsets, as documented for memory T cells challenged with chronic-infecting viruses.^{5,6,17-19}

This categorization is important, as the progenitor population seems critical to respond to CBI, by expanding and forming effector cells. Human transcriptomic studies and murine cancer and infection models support that this expanding progenitor population is characterized by expression of *TCF7*.^{5,6,20-23} However, the existence of TCF1+TRM CD8 T cells remains uncertain, as two transcription factors master of TRM formation, *HOBIT* and *BLIMP1*, have been shown to correlate with loss of *TCF7* expression.^{24,25} Similarly, *TCF7* seems to negatively regulate the expression of residency marker CD103, altogether suggesting that CBI-responding TCF1+CD8+ T cells are distinct from CBI-responding canonical TRM CD8 T cells.^{26,27} On the contrary, other studies support the coexpression of the TRM program and *TCF1/TCF7*, and we have recently identified a TCF1+CD103+CD8+ population in the tumor stroma of murine melanoma.²⁸⁻³² Overall, these data pose an intriguing avenue for further exploration, particularly when aiming to thoroughly dissect the populations responding to CBI to tailor strategies to non-responding patients.

In the intricate orchestration of immune responses, the role of antigen-presenting cells is paramount. Classic dendritic cell type 1 (cDC1), with their ability to adeptly cross-present antigens to CD8+T cells, occupy a central position in triggering effective anti-tumor response.³³ In mouse knockout of *BATF3* that cannot form cDC1, anti-tumor CD8 cytotoxic responses are abated.³⁴ Anti-PD1 treatment plus FLT3L stimulation expands cDC1 and protects mice against melanoma rechallenge.³⁵ We and others have shown that the abundance of tumor-infiltrating cDC1 correlates with favorable clinical outcomes in melanoma patients.³⁶⁻³⁸ Overall, these studies support the importance of cDC1 in cancer control. However, the participation of cDC1 in cancer control on CBI treatment has not been demonstrated.

Leveraging multiparametric proteomic approaches, this study unveils the significance of TRM CD8 T cells and cDC1, demonstrating their correlation with disease prognosis and with responding patients to immunotherapy. Notably, within the TRM CD8 T cells, we identified TCF1+ and TCF1- subsets, both exerting protective effects. Our study also reveals a transformative shift in the TRM subsets as patients progress to metastasis, particularly TCF1- TRM acquire heightened expression of checkpoint inhibitory receptors and diminish expression of effector and tissue residency markers. Essentially, this study provides a thorough examination of the complex dynamics within cancer-protective immune populations. Additionally, it underscores specific immune cells, offering valuable insights for customizing

precision immunotherapies to improve treatment effectiveness.

METHODS

Melanoma patients and control samples

This is a multicentric study involving the formation of two patient cohorts derived from the Pathology Department and/or Oncology Services of several oncology centers: Hospital de Oncología Centro Médico Nacional Siglo XXI (CMN SXXI IMSS), Hospital de Alta Especialidad 25 (IMSS), Centro Médico Nacional Manuel Ávila Camacho (IMSS), Hospital General de Zona 1A (IMSS), Centro Médico ABC, Hospital de Alta Especialidad 25 (IMSS) and Unidad Médica de Atención Ambulatoria (UMAA 199). The first cohort comprised 58 archived paraffin blocks from melanoma resection procedures while the second cohort included 24 paraffin blocks obtained before the initiation of immunotherapy. Additionally, five fresh melanoma samples were obtained from surgical resections at Hospital de Oncología CMN SXXI IMSS. Finally, eight control skin samples were derived from archived paraffin blocks, and five were obtained from fresh biopsies. All control skin samples were from patients who underwent surgeries unrelated to autoimmune/inflammatory disorders or cancer. See online supplemental tables 1 and 2 for the patient's clinical description.

Cultures of biopsies

Skin was cultured in supplemented RPMI 1640 medium (see online supplemental table 3 for a description of all used reagents, material, equipment and software). After a 7-day incubation period, cells that migrated from the skin were harvested, washed, and cryopreserved for future assays. TILs were obtained using a previously described method.³⁷ Briefly, the tumor was finely minced and incubated with 400 (U/mL) Collagenase IV and (5 mg/mL) DNase for 1 hour at 37°C. Next, enzymatic digestion was stopped by adding 0.5 μM EDTA, and digested tissues were filtered through a 70 μm strainer. After that, the cell suspension was treated with 0.2 mg/mL DNase. The lymphocyte interface of the centrifuged Percoll 40/90 solution was recovered, washed, and cryopreserved.

Immunofluorescence staining

Three μm tissue sections were affixed to electrocharged slides. Slides underwent paraffin removal, tissue rehydration, antigen retrieval, permeabilization and were incubated overnight with the respective primary antibodies. Subsequently, secondary antibodies were incubated for 2 hours. Nuclei were stained with Hoechst for 10 min and mounted with Vectashield. For multiplexed immunofluorescence (mIF), a series of staining cycles were performed on the same slide. Unconjugated primary antibodies and labeled secondary antibodies were used in the first cycle, followed by fluorochrome-conjugated antibodies in subsequent cycles to reduce cross reactivity. Tissues were mounted with PBS-Glycerol 10%, and

confocal microscopy was employed for image acquisition. Fluorochromes were bleached using H₂O₂ (4.5%) and NaOH (24 mM) for 60 min in the presence of white light. Bleaching efficiency was confirmed under the fluorescence microscope. online supplemental file 2 shows the antibody combination of each staining with example images of the staining and bleaching steps.

Confocal microscopy

Micrographs were captured using a Nikon Ti Eclipse inverted confocal microscope with NIS Elements V.4.5.0 software, 20× (dry, NA 0.75) objective lens, and Nyquist's magnification (3.4×). Three areas with high immune infiltrate, identified through H&E staining, were selected from each patient to quantify density and percentage of all phenotypes of interest. Whole slide scanning was performed with the Acquire function of the NISV.4.5.0 software, selecting the Scan Large Image option. Automated image overlapping and further analysis were conducted using FIJI ImageJ Software.

Fluorescence images analysis

IF and mIF analyses were conducted using a previously described in-house machine learning method.³⁶ Python scripts were employed for further analysis of the obtained results. To quantify the percentage of positive cells, the total number of cells positive for a specific phenotype was divided by the total cell count in the field, multiplied by 100. Density was determined by dividing the number of cells of interest by the total area of the field. Results presented in the plots represent the median value from three distinct areas per sample or patient. For single-color overlap analysis, we show the areas of marker colocalization eliminating non-colocalized pixels to facilitate the visualization of cells and areas with marker coexpression. This was achieved using the Image Calculator function in FIJI ImageJ Software.

Histocytometry

The machine learning methodology generated individual .csv files for each field of every patient, encompassing measurements of individual cells. These files were concatenated through Python scripts and subsequently analyzed using BD FlowJo V.10.9 software. online supplemental file 2 shows all the gating strategies and establishment of expression cut-off points of all the evaluated markers.

Spatial analysis

To evaluate the spatial distribution of cell phenotypes within tumor and stromal regions, we created individual regional masks for each image by tracking the tumorous area with MART-1+ staining and concatenating masks to the Machine Learning mIF images analysis. Using histocytometry, we generated XY coordinate maps and imported each phenotype of interest along with their coordinates in the image. Distances between cytotoxic cells and apoptotic melanoma cells were measured by generating .csv files and importing them into CytoMAP software V.1.4.21. The calculate distance function was employed

to estimate distances between Casp3-p+MART-1+ cells and TCF1+ or TCF1- TRMs. To standardize the data and compare distances from different datasets, we used the Bar and Violin plot extension, standardizing the data by subtracting the means and dividing them by the SD, as detailed in the original study.³⁹

Flow cytometry staining

Cryopreserved cells underwent thawing and then were stained for spectral flow cytometry. Every single positive control was used to spectral unmix. Stopping gate: 10 000 CD3+CD45RO+CD8+ events. Approximately 100 000 total events were acquired of T cells in a Cytex Aurora spectral flow cytometer (3L, 16V, 14B, 8R). Acquired files were analyzed using Flowjo V.10.8 software. See online supplemental file 2 for the gating strategy. As we did not use protein transport inhibitors, we excluded cytokines data. For the unsupervised clustering, singlets, live, CD45RO, CD3, CD8, CD69, and CD103 positive events were down-sampled at 1000 events per sample and concatenated (4000 total events) as Flow Cytometry Standard (FCS) files and UMAP clusterization was performed with all compensated parameters except for, viability, CD45RO, CD3, CD8, CD4, CD69, and CD103. We used Euclidean approximation with 15 nearest neighbors, minimum distance of 0.5, and 2 number of components. An unsupervised clustering map was performed with Flowsom using the same compensated parameters. Heat maps and representative clusters were obtained with the Cluster Explorer plugin. Trajectory analyses were performed with the PHATE plugin with 15 nearest neighbors, decay of 15, and gamma 1 and 2 components.

PCA-based clustering

Principal component analysis (PCA) was performed using 12 variables measured in patients by IF. Data processing and normalization were conducted by using R V.4.2.2. Visualization was generated using the factoextra library.

Creation of TRM and cDC1 signatures

Transcriptomic signatures for TRM CD8 T cells and cDC1s were identified through a thorough search of RNA-seq or scRNA-seq studies in the NCBI PubMed database. After manual curation, eight studies proposing TRM CD8 T cell signatures and seven studies proposing cDC1 signatures were selected.^{40–47} Integration of these signatures revealed 36 genes shared by two or more TRM CD8 studies and 23 genes shared by cDC1 studies. Additionally, 11 TRM CD8 T cell-associated genes and 3 cDC1-associated genes were incorporated into the signature based on recent literature.^{40 48–59}

Subsequently, we conducted a correlative expression analysis of the 47-gene (TRM CD8) and 26-gene (cDC1) signatures using The Cancer Genome Atlas (TCGA) melanoma database. We processed the RNA-seq count data for normalization, and the expression of the 47 and 26 genes of interest was converted into logCPM. The GSVA V.1.46.0 R package was employed to conduct an enrichment

analysis across all TCGA melanoma samples, identifying high and low enrichment groups.⁶⁰ Enriched patients were subjected to gene expression Pearson correlation analysis using the WGCNA V.1.72-1 R package,⁶¹ revealing two clusters of genes with positive and negative correlation. From these clusters, 41 TRM CD8-associated genes and 22 cDC1-associated genes showing significantly positive correlations were selected to compose comprehensive signatures. Spearman's correlation analysis was conducted to investigate the relationship between samples enriched with TRM CD8 T cells and cDC1s.

Expression enrichment and survival association

Survival analysis and creation of Kaplan-Meier curves were performed using the survminer V.0.4.9 and survival V.3.4-0 R packages. These analyses were based on categorizing the TCGA melanoma samples into high versus low enrichment of TRM, cDC1, CD8a, CD103, and CD8a/CD103 as determined from the previous GSVA V.1.46.0 R analysis. Robustness of the results was confirmed through Cox regression analysis, which involved calculating a p value and its corresponding HR. This statistical approach was employed to compare the outcomes between the groups with high and low enrichment.

Statistical analysis

We evaluated the Gaussian distribution of all data using the D'Agostino test. For experiments involving three groups, analysis of variance with post hoc multiparametric comparison was chosen. Unpaired Student's t-test was applied for two groups with independent quantitative variables. All statistical analyses were performed using Prisma software (GraphPad V.9). Results are presented as the mean±SEM. Since spatial distance measurements did not conform to a Gaussian distribution according to the D'Agostino test, a Mann-Whitney test was employed for this data. Statistical significance: *p<0.05, **p<0.01, ***p<0.001 and ****p<0.0001.

RESULTS

Study design

We conducted a comprehensive analysis using two distinct patient cohorts (figure 1A). Cohort A included 58 paraffin-embedded tumor resection specimens from individuals diagnosed with melanoma. Among these, 24 patients were classified as disease-free (DF), while 34 patients had metastatic melanoma (M) according to the American Joint Committee on Cancer TNM system for melanoma staging.⁶² All samples were assessed at the time of diagnosis, and patients were subsequently monitored for a period of 2 years. In this context, "DF" denotes patients who remained in remission throughout the follow-up period, while the "metastatic" classification was assigned either at the time of diagnosis (n=21) or upon disease progression (n=3) during the follow-up period. All metastatic patients were combined due to observed similar behavior between both latter groups. Cohort B

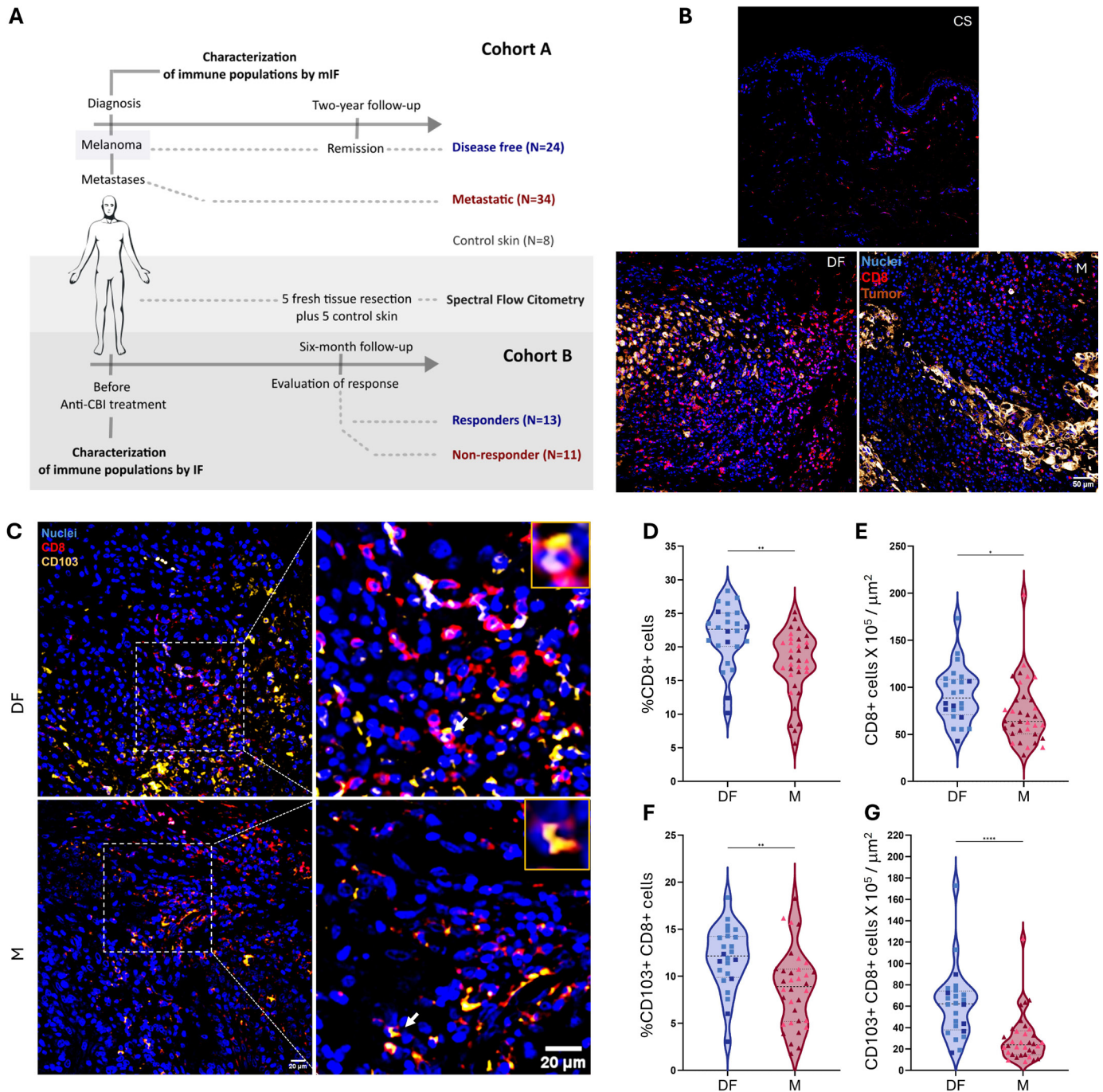


Figure 1 CD103+CD8T cells associate with disease control. (A) Diagram of study design. We included two different cohorts to examine the immune infiltrate. In cohort A, we obtained the resection products at diagnosis. Cohort A was classified into disease-free (DF) and metastatic (M) according to their clinical evolution at 2 years. In cohort B, the resection products reflect the state before treatment with CBI, and the patients were classified as responders (R) or non-responders (NR) after 6 months of follow-up. Additionally, we included five fresh tissue resections to evaluate data by spectral flow cytometry. (B–C) Immunofluorescence staining for tumor cells (MART1+, sepia), CD8 (red), CD103 (yellow), and nuclei (blue). (B) shows representative complete fields of control skin (CS), DF, and M. (C) Dotted white squares show the area selected for digital zoom in the right column. Orange squares point out examples of CD103+CD8+ cells. (D) Percentage of CD8 T cells. (E) Tissue density of CD8 per $1 \times 10^5 \mu\text{m}^2$. (F) Percentage of CD103+CD8+ T cells. (G) Tissue density of CD8+CD103+ per $1 \times 10^5 \mu\text{m}^2$. Data from DF (n=24) (light blue acral patients, dark blue non-acral cutaneous melanoma) and M (n=34) (light red acral patients, dark red non-acral cutaneous melanoma) patients. Unpaired Student's t-test, * $p < 0.05$, ** $p < 0.01$, and **** $p < 0.0001$.

comprised tissue resection specimens from 24 patients collected before CBI treatment initiation. These patients were later classified as either responders (R, n=13) or non-responders (NR, n=11) based on RECIST response

criteria, evaluated 6 months after immunotherapy commencement. Additionally, skin samples from eight individuals without neoplastic conditions served as our control group. All tissue samples underwent IF staining.

In cohort A, our analysis aimed to primarily characterize CD8 T cell and cDC1 phenotypes associated with disease control and improved prognosis. Cohort B aimed to elucidate the importance of these populations for immunotherapy response. To ensure the reliability of our findings, we analyzed five additional fresh melanoma tissues and five fresh control skins, using spectral flow cytometry, to confirm the IF phenotypes observed in situ and to more in-depth characterize protective populations.

Tumor-infiltrating CD103+ CD8 T cells are enriched in patients controlling melanoma

TILs are generally associated with improved prognoses in melanoma and other cancers. However, some patients, despite having abundant TILs, struggle to control the disease and develop metastases. This underscores the need to thoroughly characterize specific cell populations and phenotypes associated with disease control. We first focused on cytotoxic CD8 T cells, which are recognized as the primary effectors in antitumoral immune responses, and CD103 expression, a marker of tissue residency, also associated with better clinical outcomes in various cancer types.⁶³

Although the level of cellular infiltration in DF and M melanoma samples was not strikingly different (as indicated by the abundance of nuclei in [figure 1B](#)), noticeable differences were observed in the abundance and distribution of CD8 T cells. Specifically, clusters of CD8 T cells were prominently visible in DF patients, whereas M patients exhibited fewer and more dispersed T cells throughout the samples ([figure 1B,C](#)). The analysis of three highly infiltrated regions of each sample revealed that CD103–CD8+ and CD103+CD8+ populations were significantly enriched in melanoma samples and DF patients compared with control skin (online supplemental file 2) and M patients ([figure 1D–G](#)), respectively. However, the latter appeared to better distinguish between melanoma controllers and progressors. These observations were more pronounced when the data were scored as cell densities rather than percentages. These findings suggest that, while the abundance of CD8+ T cells is crucial, the CD103+CD8+ compartment seems particularly important in effectively controlling melanoma progression.

Both TCF1+ and TCF1– CD103+ CD8 T cell subsets are protective

We previously highlighted the importance of TCF1+CD103+CD8+ cells in controlling melanoma growth in a murine model.³⁰ Transcriptomic studies also support the existence of these cells.^{17 18 28 31} We assessed the abundance of these cells in tumor infiltrates from DF and M patients ([figure 2A](#), online supplemental file 2). DF patients exhibited a significant enrichment of TCF1 CD103 double positive and CD103 single positive CD8 T cells ([figure 2B](#), online supplemental file 2), while M patients showed enrichment in the CD103 negative subsets (online supplemental file 2). The percentage of

the TCF1+CD103+ CD8 T cell subpopulation relative to the total tumor-infiltrating cells yielded similar results ([figure 2C](#)). Additionally, we found an enrichment of the TCF1–CD103+CD8+ subpopulation in DF patients ([figure 2B,D](#)). Evaluating the prognostic potential of both TCF1+ and TCF1– CD103+ CD8 subsets in relation to tumor staging revealed decreased percentages in advanced melanoma stages, emphasizing their significance in stages with favorable prognosis (see [figure 2E,F](#)).

Enrichment of cDC1 also characterizes melanoma controllers

Due to their crucial role in fostering the presence and activation of T cells, we next investigated cDC1 infiltration and association with CD103+ CD8 T cells. Our findings in this independent and larger cohort corroborated previous observations of the positive correlation between cDC1 and disease control (see online supplemental file 2). To reinforce our findings identifying CD103+ CD8 T cells and cDC1 associated with disease control, we compiled a comprehensive database based on our immune assessment of cohort A. This database comprised 12 variables, encompassing percentages and phenotypic compositions of immune cell subsets, along with the differentiation between DF and M outcomes. Hierarchical heatmap visualization revealed two distinct clusters, with the DF-associated cluster including the three protective populations, and the M-associated cluster composed of CD103–negative CD8 T cell subsets (see online supplemental file 2). Employing a PCA-based clustering approach, we further confirmed that CD103+CD8+ subsets and cDC1 subsets clustered with DF patients, while CD103– CD8+ subsets clustered with M patients ([figure 2G](#)). These findings support the association of both TCF1+ and TCF1– CD103+ CD8 T cells and cDC1 with melanoma control. Notably, [figures 1D–G](#), and [2C–G](#), and online supplemental file 2 highlight acral melanomas, revealing an equal distribution between DF and M patients. These findings support the notion that both TCF1+ and TCF1– CD103+ CD8 T cells, along with cDC1 cells, also play protective roles in this melanoma subtype.

CD103+ CD8 T cells are bona fide TRM T cells

Recent studies have emphasized the role of TRM CD8 T cells as a key immune population associated with cancer control across various solid tumors. CD103 acts as a ligand for E-cadherin, anchoring T cells to epithelial tissue, making CD103 expression indicative of tissue residence. We aimed to thoroughly characterize the phenotype of CD103+ CD8 T cells to unequivocally establish their identity as TRM cells and confirm the evidence that both TCF1+ and TCF1– CD103+ CD8 T cell subsets correlate with disease protection. Given previous findings suggesting that CD103 and TCF1 expression might be mutually exclusive, we conducted a mIF analysis using nine protein markers and nuclei to confirm tissue residency in a subset of patients from cohort A (n=10). The additional markers included CD69, HOBIT and RUNX3 to confirm tissue residence, and CD45RO as a marker of

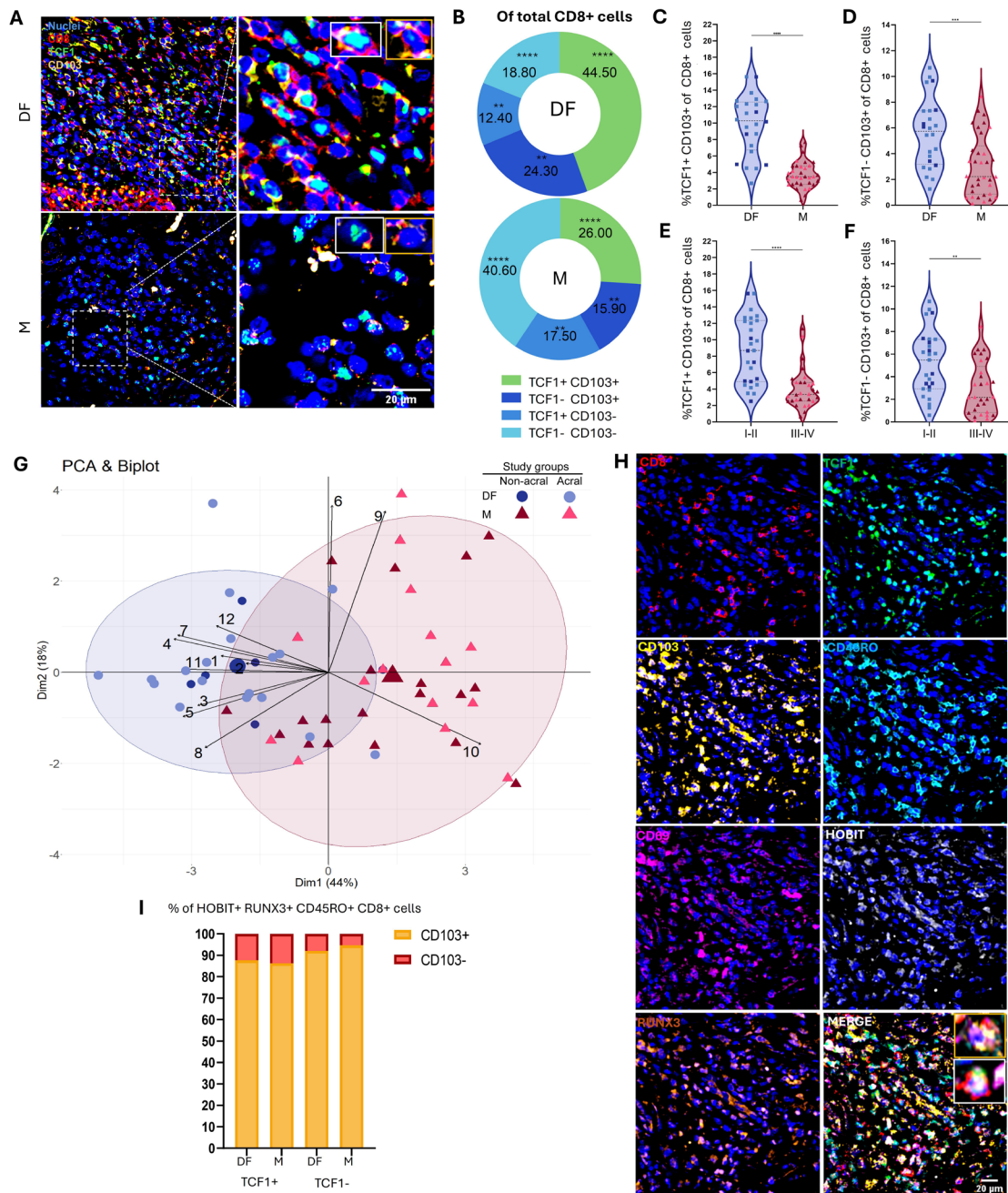


Figure 2 CD103+ CD8 T cells are bona fide TRM cells and both TCF1- and TCF1+ subsets are protective. (A) Representative micrographs of immunofluorescence (IF) staining for TCF1 (green), CD103 (yellow), CD8 (red), and nuclei (blue). Dotted white squares show the area selected for digital zoom in the right column. White squares point out to an example of TCF1+CD103+ CD8T cells, and yellow squares point out to TCF1- CD103+CD8T cell. (B) Pie charts depicting the distribution of TCF1 CD103 CD8 phenotypes related to the total CD8 fraction. (C-F) Percentages of TCF1+ and TCF1- CD103+CD8T cell populations. (C, D) Disease-free (DF) patients are in blue and metastatic (M) patients are in red. (E, F) Stage I and II (blue) and stage III and IV (red). (G) PCA plot, each blue dot represents a DF patient (n=24), and red triangles represent M patients (n=34). The resulting grouping was obtained by PCA of 12 immune cell population measurements. As a result, each measurement is denoted by black vectors with the corresponding match number from vectors: 1 (%CD8+), 2 (CD8+ tissue density), 3 (%CD103+CD8+), 4 (%TCF1+CD103+CD8+), 5 (%TCF1- CD103+CD8+), 6 (%TCF1+CD103- CD8+), 7 (%TCF1+CD103+ CD8+ of total CD8+ cells), 8 (%TCF1- CD103+CD8+ of total CD8+ cells), 9 (%TCF1+CD103- CD8+ of total CD8+ cells), 10 (%TCF1- CD103- CD8+ of total CD8+ cells), 11 (%cDC1 cells with respect to the total infiltrate) and 12 (%CD11c with respect to the total infiltrate). (C-G) Acral melanoma is presented in light blue (DF plots) or light red (M plots), non-acral cutaneous melanoma is presented in dark blue (DF plots) and dark red (M plots). (H) Multiplex immunofluorescence staining for CD8 (red), TCF1 (green), CD103 (yellow), CD45RO (cyan), CD69 (magenta), HOBIT (gray), RUNX3 (orange), and nuclei (blue). Squares point to CD103+CD69+ HOBIT+ RUNX3+CD8+ CD45RO+TCF1+ cells (white) and TCF1- cells (yellow). (I) Quantification of CD103+ cells on HOBIT+RUNX3+ CD45RO+CD8+ fraction, in both TCF1+ and TCF1- subsets. Unpaired Student's t-test, **p<0.01, ***p<0.001 and ****p<0.0001.

previous antigenic exposure and memory (figure 2H). We leveraged an artificial intelligence algorithm and histocytometry for quantification and visualization of mIF data (online supplemental file 2). We observed that nearly 100% of CD103+ cells were positive for the additional tissue residency and memory markers, irrespective of TCF1 expression status (figure 2I). This comprehensive analysis provided compelling evidence that the CD103+ CD8 T cells associated with disease control indeed represented TRM cells.

TRM CD8 and cDC1 signatures are associated with survival in the TCGA melanoma database

We explored the clinical relevance of tissue residency evaluating its influence on the survival of melanoma patients. We initially examined the survival outcomes of TCGA melanoma patients (n=472) based on high expression levels of the following markers: *CD8*, *CD103*, *CD8* and *CD103* combined, and the gene signature of cDC1 (*CD11c*, *HLADR*, and *BDCA3*). This analysis revealed an association between enhanced survival and increased expression of these markers, particularly CD8 and cDC1 (online supplemental file 2). We also constructed extended TRM and cDC1 transcriptional signatures (online supplemental file 2). The enrichment of the signatures significantly correlated with improved overall survival probability (TRM Kaplan-Meier $p=2.46 \times 10^{-6}$; cDC1 $p=3.84 \times 10^{-6}$) (figure 3A), while the combination of both signatures raised the p value to 3.48×10^{-7} . Notably, the p value of the TRM signature was significantly more robust than that of *CD8*-high expressors and *CD103*-high expressors (online supplemental file 2). Altogether, these findings underscore the pivotal role of TRM CD8 T cells in influencing patient outcomes, even when both subsets are compared within patients with high level of infiltration of CD8 T cells (online supplemental file 2).

TRM T cell subsets are in close proximity with cDC1s in tumor and stromal regions

We assessed the spatial relationship between TRM T cells and cDC1s within melanoma and examined whether these immune cells exhibited close proximity suggestive of cell-to-cell interactions. Using mIF staining, we identified TCF1+ and TCF1- TRM CD8 T cells, cDC1s, and melanoma cells. Four whole slides from both DF and M patients were randomly selected and scanned, enabling the generation of topological maps delineating tumor and stromal regions (figure 3B and online supplemental file 2). Our analysis revealed that these immune cell populations were predominantly localized in stromal areas surrounding the tumor. Figure 3B shows an image illustrating single-color representations of TRM T cells, cDC1s, and melanoma cells, demonstrating examples of two-way and three-way cell interactions involving TCF1+ or TCF1- T cells with melanoma cells, as well as TCF1+ or TCF1- T cells with cDC1s and melanoma cells (middle panel). A representative image illustrates the close interactions between TCF1+ TRM CD8, cDC1 and

melanoma cells (bottom panel). TCF1- T cells (19.8%) and cDC1s (26.6%) appear to exhibit greater enrichment in tumorous areas compared with TCF1+ T cells (14%) (figure 3C). To explore the relationship between TCF1+ and TCF1- CD103+ CD8+ T cells and cDC1s, we conducted a simple linear regression analysis involving all patients from cohort A, observing positive and significant correlations (figure 3D). We also observed a high correlation in patients from the TCGA database (figure 3E). These findings provide compelling evidence for close interactions between both TCF1+ and TCF1- subsets of CD103+ CD8 T cells with cDC1s and tumor cells, suggesting that these three immune populations are controlling the tumor growth.

Melanoma controllers harbor more functionally active TRM T cells

While confirming the TRM nature of CD103+ CD8 T cells, we observed differences in the expression of tissue residence-related genes between TCF1-positive and TCF1-negative subsets. The former exhibited varying levels of marker expression, identifying a RUNX3-high population that was absent in their TCF1- counterparts (online supplemental file 2). A similar pattern of expression was observed for HOBIT (online supplemental file 2), indicating intrinsic lower levels of tissue residency markers for the TCF1- CD103+ CD8 T cells.

We conducted a detailed exploration of the differences between TRM subsets, analyzing their effector-function potential and its implications for disease control. We evaluated the expression of the checkpoint inhibitor PD1, the antitumoral cytokine IFN- γ , and the proliferation marker Ki67 (figure 4A and online supplemental file 2). Notably, more than 80% of cells in both TCF1 subsets expressed PD1, suggesting similar states of exhaustion (online supplemental file 2). Initially defined as an unresponsive, terminal state, exhaustion has been redefined through subsequent research, revealing a continuum of states marked by varying levels of effector activities. Gating on the PD1+ TRM subset, we observed that TCF1+ cells not only expressed higher levels of IFN- γ and Ki67, but also harbored a greater number of cells positive for these markers than TCF1- cells, supporting a higher proportion of functionally active cells within this subset (figure 4B and online supplemental file 2). Strikingly, we observed higher levels of both IFN- γ and Ki67 in both TCF1+ and TCF1- TRM subsets in DF patients than in M patients (figure 4C,D). In summary, our results suggest that while the TCF1+ TRM CD8 T cells display enhanced functionality compared with the TCF1- cells, both subsets seem functional since both express effector molecules. While present in low numbers, TRM CD8 T cells in M patients still harbor IFN- γ + and Ki67+ effector cells.

Cytotoxic TCF1- TRM CD8 T cells associate with apoptotic melanoma cells

After observing the apparent functional differences between TCF1+ and TCF1- TRM subsets, we explored

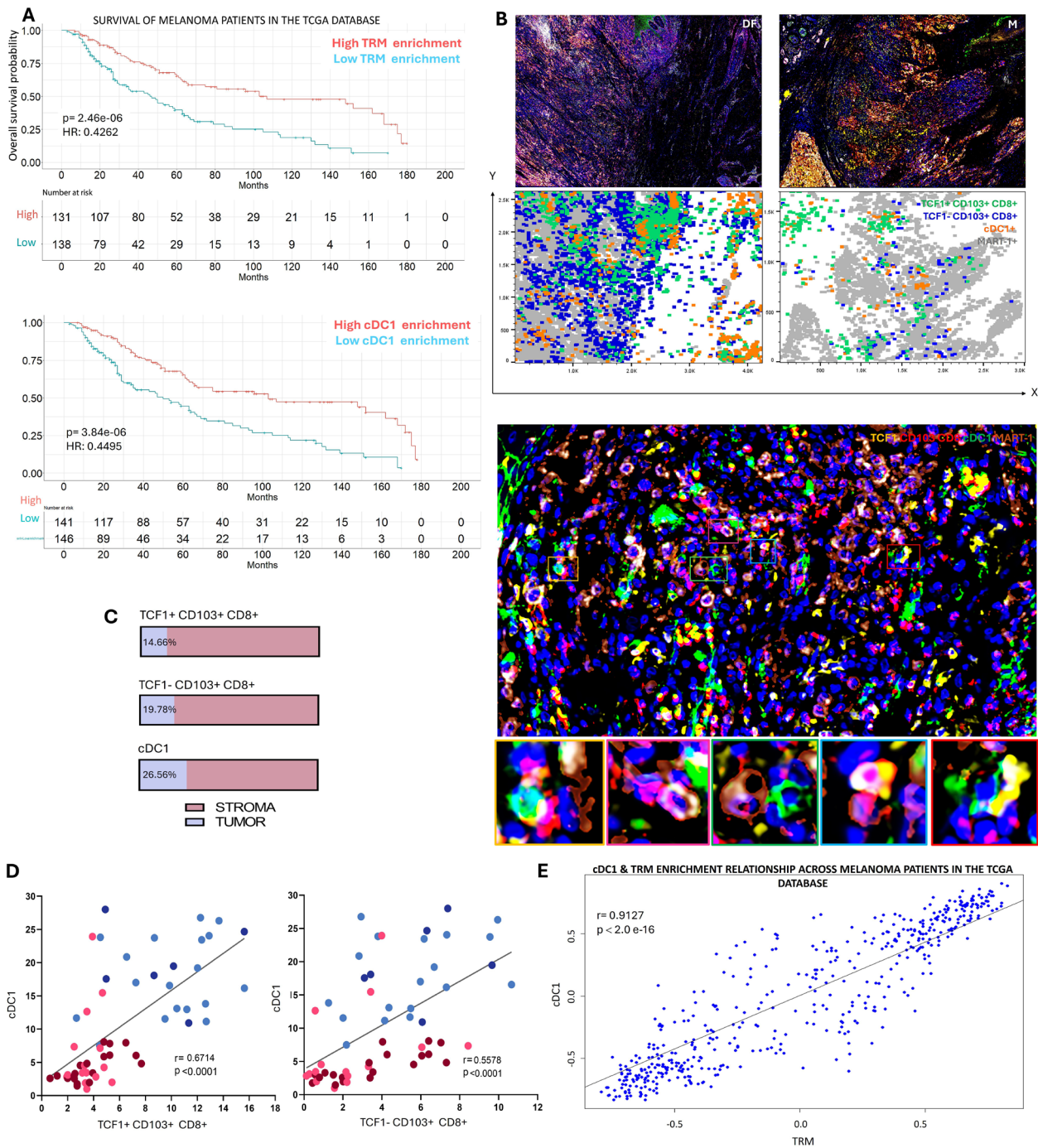


Figure 3 There is a high correlation between the enrichment of TRM CD8 T cells and cDC1, which is associated with patient survival. (A) Kaplan-Meier survival curves for TRM CD8 T cells (top) and dendritic cell type 1 cDC1 (bottom). Curves show a comparison over the course of 180 months between high versus low enrichment samples. For both populations high enrichment is associated with a better patient survival probability, as demonstrated by the HR and p value obtained from Cox regression. (B) Whole slide images of IF staining for TCF1 (green), CD103 (yellow), CD8 (red), CD11c (magenta), HLA-DR (gray), BDCA-3 (yellow hot), MART-1 (sepia), and nuclei (blue) of representative DF and M patients (top). For the topological maps (middle) representing the X and Y coordinates, all colors were merged as follows: of TCF1+CD103+ CD8 (green), TCF1- CD103+CD8 (blue), cDC1 (orange), and tumor cells (gray). Each point represents one cell. Micrograph (bottom) showing single-color overlap analysis of CD103+CD8+ (red), TCF1 (orange), cDC1 (green), and MART-1 (sepia). In squares of different colors, we show the three way interactions between TCF1- and TCF1+ TRM CD8s, cDC1s, and tumorous cells. To visualize the whole slide images see online supplemental file 2. (C) Bar graphs depicting the percentage of cells localized on intratumorally or stromal areas defined by MART-1 expression. (D) Simple linear regression and Spearman's correlation test for %TCF1+CD103+ CD8+ vs %cDC1 (left) and %TCF1- CD103+CD8+ vs %cDC1 (right). (E) TRM and cDC1 enrichment association across melanoma patients in the TCGA database is presented by a linear regression analysis.

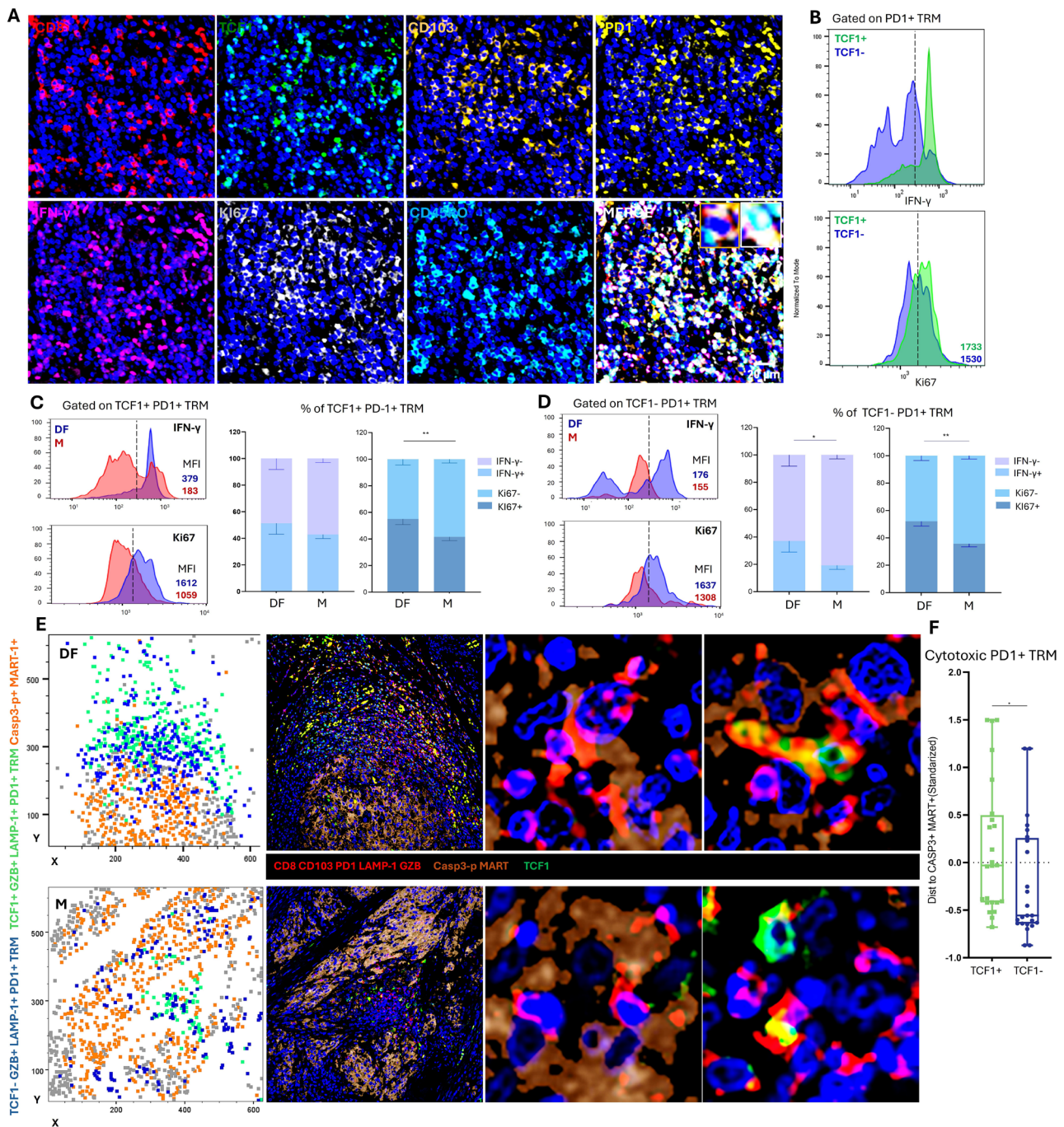


Figure 4 TCF1+ and TCF1- TRM CD8 T cells exhibit differential functional features. (A) Multiplex immunofluorescence (mIF) staining for CD8 (red), TCF1 (green), CD103 (yellow), PD1 (bright yellow), IFN- γ (magenta), Ki67 (gray), CD45RO (cyan) and nuclei (blue), white square points out to an example of a TCF1+ and yellow square to a TCF1- cell. (B) Histogram (top) showing the mean fluorescence intensity (MFI) of IFN- γ (top) and Ki67 (bottom) of TCF1+ (green) and TCF1- (blue) subsets gated on PD1+ TRM cells. (C, D) Histograms and bar graph showing the MFI and proportion, respectively, of IFN- γ + and IFN- γ -, and Ki67+ and Ki67- cells in the fraction of PD1+ TRM CD8 T cells that are TCF1+ (C) and TCF1- (D). Patients are divided in disease-free (DF, n=5) and metastatic (M, n=5). (C, D) Thresholds to assign positive and negative cells for IFN- γ and Ki67 are shown in online supplemental file 2. (B–D) Concatenated data of the 5 DF and 5 M datasets. (E) Whole slide images of mIF staining representing PD1+ TRM CD8 cells, marked as TCF1- or TCF1+, apoptotic melanoma cells, phosphorylated caspase 3+ and nuclei of representative DF and M patients. Topological maps are shown in the left panels while mIF images in the right panels. For the left topological map each point represents one cell and populations are marked as GZB+LAMP-1+ PD1+ TRM CD8 cells: TCF1- (blue) and TCF1+ (green), and MART-1+Casp3-p+ apoptotic melanoma cells (sepia). mIF also shows single-color overlap analysis of these cells. Here, GZB+LAMP-1+ PD1+ TRM CD8 cells: TCF1- (are marked as red) and TCF1+ (green), and MART-1+Casp3-p+ apoptotic melanoma cells (sepia), see also online supplemental videos 1 and 2. (F) Distance of TCF1+ and TCF1- PD1+ TRM to apoptotic melanoma cells. Unpaired Student's t-test, *p<0.05 and **p<0.01.

their cytolytic potential and their spatial proximity to melanoma cells. We randomly selected four DF and four M patients for mIF staining of GZB+ (granzyme B) and LAMP-1+ (lysosomal associated membrane protein 1) markers, indicative of cytotoxicity potential within the PD1+TRM subsets. Additionally, Casp-3-p (phosphorylated caspase 3) and MART-1 markers were assessed to determine whether cytotoxic cells were spatially associated with apoptotic melanoma cells. We observed that GZB+LAMP-1+ PD1+ cells were enriched in the TCF1-TRM subset, with DF patients showing a higher proportion (64%) compared with M patients (47%) (online supplemental file 2). Since this analysis considered the entire field without regard to tumor location, we generated XY coordinate plots to assess spatial associations between cytotoxic TRM subsets and apoptotic melanoma cells. The TCF1- subset was enriched in tumor areas, exhibiting closer proximity to Casp3-p+MART-1+ cells (figure 4E and online supplemental file 2). Image processing facilitated the visualization of interactions between cytotoxic cells and apoptotic melanoma cells (figure 4E and supplemental videos 1-2). Distance estimation between Casp3-p+MART-1+ cells and cytotoxic TRM subsets revealed that the TCF1- population was significantly closer to apoptotic tumor cells, supporting a more direct involvement in tumor cell death (figure 4F).

TCF1- TRM T cells accumulate exhaustion markers in metastatic patients

Exhausted populations have been recognized to transition from a progenitor-like population expressing TCF1 to a more terminally exhausted population, characterized by negativity for TCF1 and positivity for inhibitory checkpoint receptors PD1, TIM3, LAG3, CTLA4, and CD39. Given the prevalent expression of PD1 in TRM CD8 T cells, we explored whether the TCF1-positive and TCF1-negative TRM subsets might exhibit signs of terminal exhaustion. To investigate this, we assessed the expression of PD1, TIM3, the exhaustion-associated transcription factor TOX, and CXCR5, a marker of functionality among exhausted cells and of positive response to CBI (figure 5A and online supplemental file 2). Our analysis revealed that both TCF1+ and TCF1- TRM subsets contained exhausted cells coexpressing PD1 and TOX (figure 5B). The TCF1+ population displayed higher levels of CXCR5 expression and a greater proportion of CXCR5-positive cells, aligning more closely with a progenitor-like effector state while the TCF1- population exhibited higher expression of TIM3 and more TIM3+ cells, indicative of a more terminally exhausted state (figure 5C).

Further investigation into the differences in exhaustion profiles between DF and M patients revealed that TCF1+ TRMs from M patients exhibited slightly higher expression of exhaustion markers PD1, TOX and TIM3 (figure 5D left). When we evaluated the PD1+TOX+ subset, we observed a higher frequency of CXCR5+ cells in DF patients and of TIM3+ cells in M patients (figure 5D right). These differences were significantly more

pronounced within the TCF1- TRM subset, with TIM3 expression notably elevated in these cells in M patients (figure 5E). These results indicate that both TRM subsets in M patients exhibit a higher degree of exhaustion compared with their DF counterparts, with TCF1- TRM appearing more exhausted than TCF1+ TRM.

Spectral cytometry supports the association of TCF1+ TRM with melanoma control

To validate our mIF findings and to further delineate phenotypic differences among TRM subsets in DF and M melanoma patients, we conducted single-cell analysis using 25-parameter spectral flow cytometry focusing on CD8 TRM (figure 6A). For this, we obtained T cells from five fresh melanoma samples and five control skin samples. online supplemental file 2 shows the strategy of CD8 TRM gating and compensation. We observed higher percentages of CD69+CD103+ CD8 TRM T cells in melanoma patients than in control skins (online supplemental file 2). Comparing TCF1+ and TCF1- TRM subsets confirmed that TCF1+ cells were enriched in RUNX3+ and Ki67+ cells, while TCF1- cells showed enrichment in PD1 and TIM3 (figure 6B). Further exploration of effector and exhausted states in patients revealed that TRM CD8 T cells from DF patients exhibited lower expression of exhaustion markers but higher expression of Ki67, and CXCR5 (figure 6C). Interestingly, although TRM CD8 T cells from M patients express more exhaustion markers, they also express more of the cytotoxic proteins (online supplemental file 2). These data corroborated the mIF findings, indicating that TCF1+ TRM cells exhibit enhanced proliferative and effector potential while TCF1- TRM cells appear more exhausted. Furthermore, DF patients are enriched with effector cells while M patients exhibit terminally exhausted CD8 TRM cells.

To investigate the trajectory between TCF1+ and TCF1- subsets, we employed an unsupervised approach using the PHATE algorithm following UMAP dimensional reduction, including the 25 markers from spectral flow cytometry (online supplemental file 2). This analysis suggested that TCF1+ TRM cells give rise to exhausted TCF1- TRM CD8 T cells, a trajectory that seems more active in M patients, potentially leading to a loss of control over melanoma growth and spread. These findings align with recent studies documenting a progenitor state of TCF1+ cells, giving rise to more effector T cell populations that eventually become terminally exhausted in conditions of chronic antigenic stimulation, such as cancer or viral infection, setting the stage for disease progression.

Dimensional reduction revealed differential clustering among samples (figure 6D and online supplemental file 2), and the FlowSOM algorithm identified five distinct clusters (C0-C4) differentially enriched among samples. C0, abundant in control skin, displayed discrete expression of exhaustion and effector markers, suggesting a non-activated homeostatic state. C1, enriched in DF, exhibited high expression of TCF1, RUNX3, Ki67, and CXCR5, with low expression of most exhaustion markers.

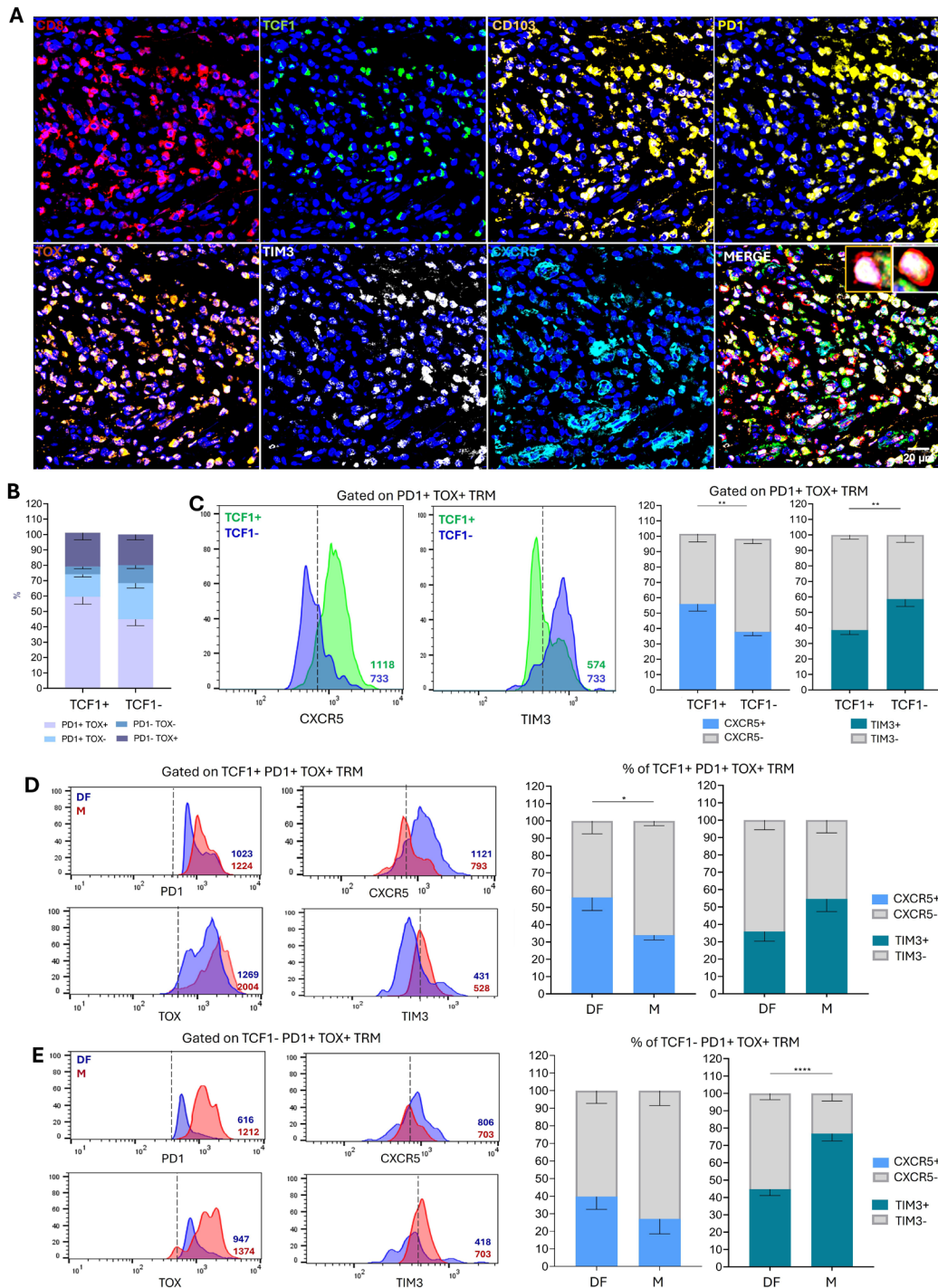


Figure 5 Exhausted phenotypes TCF1+ and TCF1- TRM CD8 T cell subsets and their association with disease control. (A) Multiplexed immunofluorescence (mIF) staining for CD8 (red), TCF1 (green), CD103 (yellow), PD1 (bright yellow), TOX (orange), TIM3 (gray), CXCR5 (cyan), and nuclei (blue), white square points out to an example of a TCF1+ and yellow square to a TCF1- cell. (B) Bar graph showing the proportion of PD1+TOX+, PD1-TOX+, PD1-TOX-, and PD1-TOX- cells in the fraction of TCF1+ and TCF1- TRM CD8 T cells (CD103+CD45RO+CD8+). (C) Histogram (left) showing the mean fluorescence intensity (MFI) of CXCR5 and TIM3 of TCF1+ (green) and TCF1- (blue) cells, gated on PD1+TOX+ TRM CD8 T cells. Bar graph (right) showing the proportion of CXCR5+ and CXCR5-, and TIM3+ and TIM3- cells in the fraction of PD1+TOX+ TRM CD8 T cells that are TCF1+ and TCF1-. (D) Histograms (left) showing the MFI of PD1, CXCR5, TOX, and TIM3, of TCF1+ TRM CD8 T cells in disease-free (DF blue, n=5) and metastatic (M red, n=5) patients. Bar graph (right) showing the proportion CXCR5+ and CXCR5-, and TIM3+ and TIM3- cells in the fraction of TCF1+PD1+ TOX+ TRM CD8 T cells. (E) Like (D) but in TCF1- TRM CD8 T cells. (C–E) Thresholds to assign positive and negative cells for CXCR5 and TIM3 are shown in online supplemental file 2. (B–E) Concatenated data of the 5 DF and 5 M datasets. Unpaired Student's t-test, * $p < 0.05$, ** $p < 0.01$, and **** $p < 0.0001$.

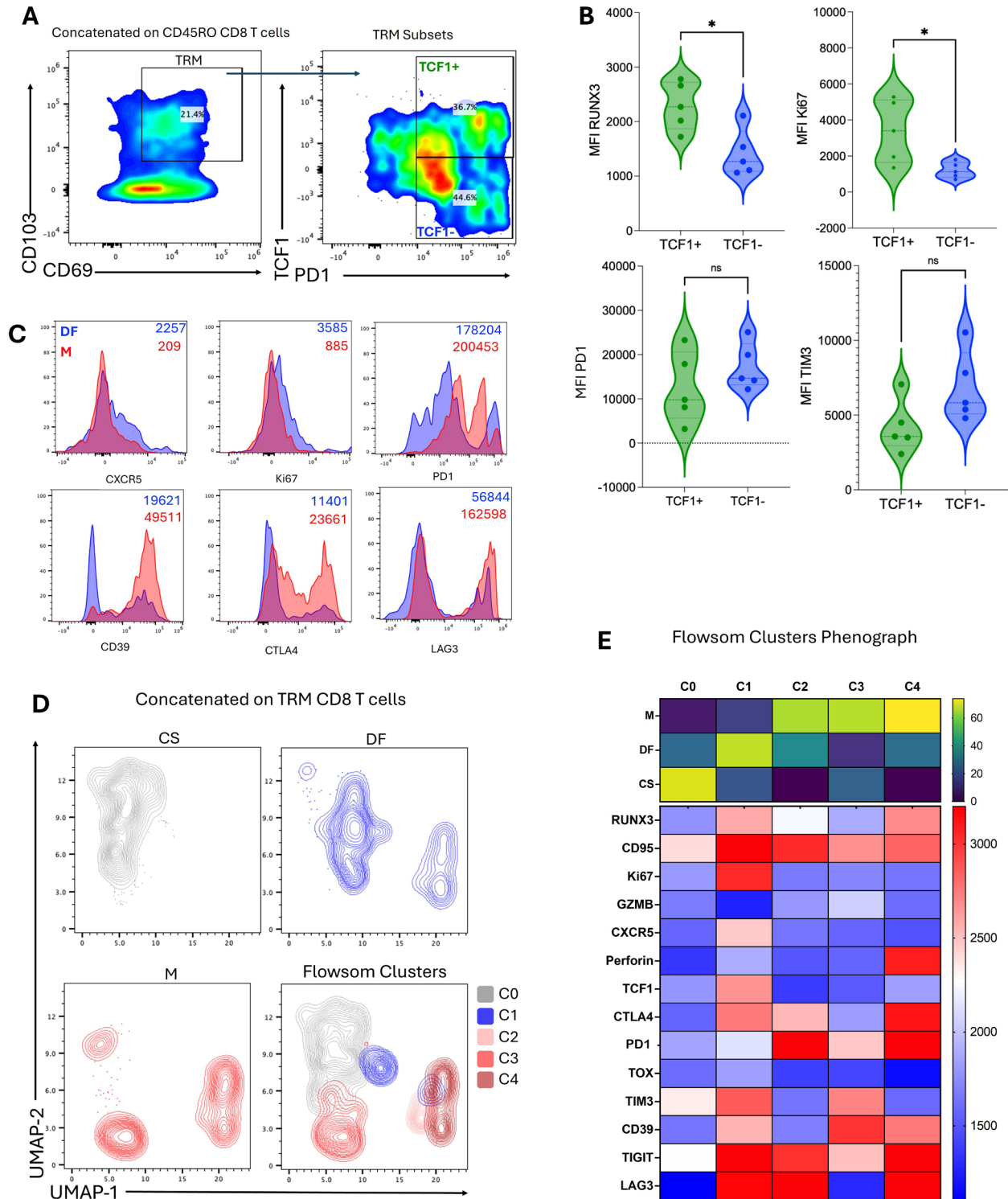


Figure 6 Spectral flow cytometry validates the protection of TCF1+ TRMCD8 T cells and the shift to a more exhausted TCF1- cell in metastatic patients. Tumor-infiltrating lymphocytes were obtained by enzymatic digestion of fresh melanoma tumor samples and were stained for spectral flow cytometry. Phenotypic changes in TRM CD8 T cells from control skin (CS) or melanoma samples were analyzed. (A) Representative dot plots showing percentages of TRM CD8 T cells (CD69+CD103+CD8+) in fresh melanoma tumor samples. (B) Violin plots showing quantification of mean fluorescence intensity (MFI) of RUNX3, Ki67, PD1, TIM3 in TCF1+PD1+ and TCF1- PD-1+ TRMCD8 T cells. (C) Histograms showing expression of CD39, CTLA4, LAG3, PD1 and CXCR5, for these histograms TRM CD8 T cells among all DF or M patients were concatenated. (D) UMAP clusterization of TRM CD8 T cells from all samples, showing CS (gray), DF (blue), M (red), and Flowsom aggrupation of TRM CD8 T cells. (E) Phenograph heatmap from populations identified by the Flowsow algorithm and its sample enrichment. Data from n=5CS, and n=5 melanoma samples, 600–800 TRM CD8 T cells (CD69+ CD103+) events from each sample were concatenated and analyzed. The IQR and median are shown in dotted lines in violin plots, t-test and Welch's correction were used to determine statistical differences among DF and M patients, *p<0.05.

In contrast, C2 to C4, enriched in M patients, displayed higher expression of all exhaustion markers and poor expression of Ki67, CXCR5, TCF1, and RUNX3, indicating a compromised functional state of TRM CD8 T cells in M patients (figure 6E). Pearson's correlation analysis revealed a strong correlation between Ki67, CXCR5, and TCF1 in TRMs CD8 T cells from DF patients, and CTLA4, PD1, CD39, and TIM3 in TRM cells from M patients (online supplemental file 2). In summary, spectral flow cytometry data support differentially activated states in TRM CD8 T cells within melanoma samples from DF and M patients, with a more effector phenotype in the former and a more exhausted phenotype in the latter.

TCF1+ and TCF1– TRM subsets and cDC1 are enriched in CBI responders

Current guidelines advocate for checkpoint inhibitors immunotherapy as the primary treatment for advanced and metastatic melanoma.⁶⁴ This approach has sparked interest in identifying responsive immune populations, aiming to tailor and enhance therapeutic responses, ultimately benefiting a broader spectrum of patients. We explored the potential connection between TCF1-positive and TCF1-negative TRM populations and their response to immunotherapy. We observed both TCF1+CD103+ CD8+ and TCF1–CD103+CD8+ subsets present in higher percentages and densities in patients who responded to immunotherapy (R) compared with non-responders (NR) (figure 7A–C). In contrast, CD103– CD8 T cells were enriched in NR patients. We also observed significantly more cDC1 in R patients than in NR patients (figure 7D,E). Additionally, we conducted a PCA-based clustering analysis. Despite the limited sample size, this analysis effectively segregated R and NR patients, with CD103+ CD8 TRM and cDC1 populations closely associated with DF patients (figure 7F). These data strongly suggest that CD103+CD8 TRM are closely associated with a positive response to immunotherapy, and both TCF1+ and TCF1– subsets contribute to this response. It is noteworthy that this evaluation represents the composition of the immune infiltrate before the initiation of treatment, emphasizing the relevance of the pretreatment immune infiltrate in influencing therapeutic response. A correlative analysis of these populations further confirmed their close association (figure 7G). Interestingly, in CBI-treated patients, there appeared to be an enhanced correlation between cDC1s and the most cytotoxic TRM subtype ($r=0.855$), compared with the same correlation observed in CBI-naïve patients ($r=0.5578$), perhaps reflecting the CBI-induced restoration of antitumor functions. Collectively, these data underscore the crucial roles of TRM and cDC1 in melanoma control, making them valuable targets for immunotherapy aimed at restoring their effector functions.

DISCUSSION

While melanoma stands as one of the primary targets for CBI utilization, it remains a significant threat as the most lethal form of skin cancer, with escalating incidence and mortality rates in Latin America, Asia, and Africa.⁶⁵ In this study, our objective was to characterize the contribution of TRM CD8 T cells and cDC1s in melanoma control, improved prognosis, and favorable response to immunotherapy. The outcome of this investigation provides valuable insights into immune cells fundamental for disease prognosis and for customizing precision immunotherapies.

We observed TRM CD8 T cells and cDC1 as protective against melanoma growth, not only in CBI-naïve patients but also in CBI-treated. TRM CD8 T cells exhibited superior protection compared with CD8 T cells, as evidenced in our patient cohorts and the TCGA melanoma database. We validated these cells as bona fide TRM through the expression of tissue residency markers CD103 and CD69, along with CD45RO, RUNX3, and HOBIT. Intriguingly, we identified two protective TRM subsets, TCF1+ and TCF1–, with the former displaying an apparent enhanced capacity for proliferation and IFN- γ production while the latter exhibiting an apparent heightened cytotoxicity. In metastatic patients, both TRM subsets accumulated exhaustion markers, particularly the TCF1– subset, which also lost expression of tissue residency markers. We do not know the fate of the exhausted TCF1– TRM cells, loss of the residency program may indicate tissue egression. Importantly, both subsets expressed PD1 in more than 80% of cells. Indeed, we observed that TCF1– TRM cells in M patients still harbored cells positive for IFN- γ , Ki67 and cytotoxic molecules, in addition to the accumulative expression of PD1, CTLA4, TIGIT, LAG3, TIM3, and CD39, rendering them an ideal target for recovering effector functions through CBI.

It is documented that cDC1s form clusters with CD8 T cells promoting their activation, expansion, differentiation, and cancer protection.⁶⁶ Similarly, we observed a close spatial proximity between TRM CD8 T cells and cDC1s, along with a strong correlation in the abundance of both cell populations. This evidence underscores steady functional interactions between both immune cells. The preferential interactions observed between TCF1+ TRMs and cDC1s in the tumor stroma of CBI-naïve patients, potentially reflect on their known antigenic priming role. Interestingly, the heightened interactions between TCF1– TRMs and cDC1s observed in the tumor regions of patients treated with CBI may also suggest a continuous need for cDC1s to sustain T cell cytotoxic effector functions. This idea is also bolstered by the finding that TCF1– TRMs CD8 T cells are predominantly associated with apoptotic melanoma cells.

We have previously documented the protective role of cDC1s in melanoma.^{36,37} This is favored by studies demonstrating the necessity of cDC1s for effective CD8 T cell activation, as evidenced by the absence of protective CD8 T cell responses in mice lacking cDC1. Additionally, mice

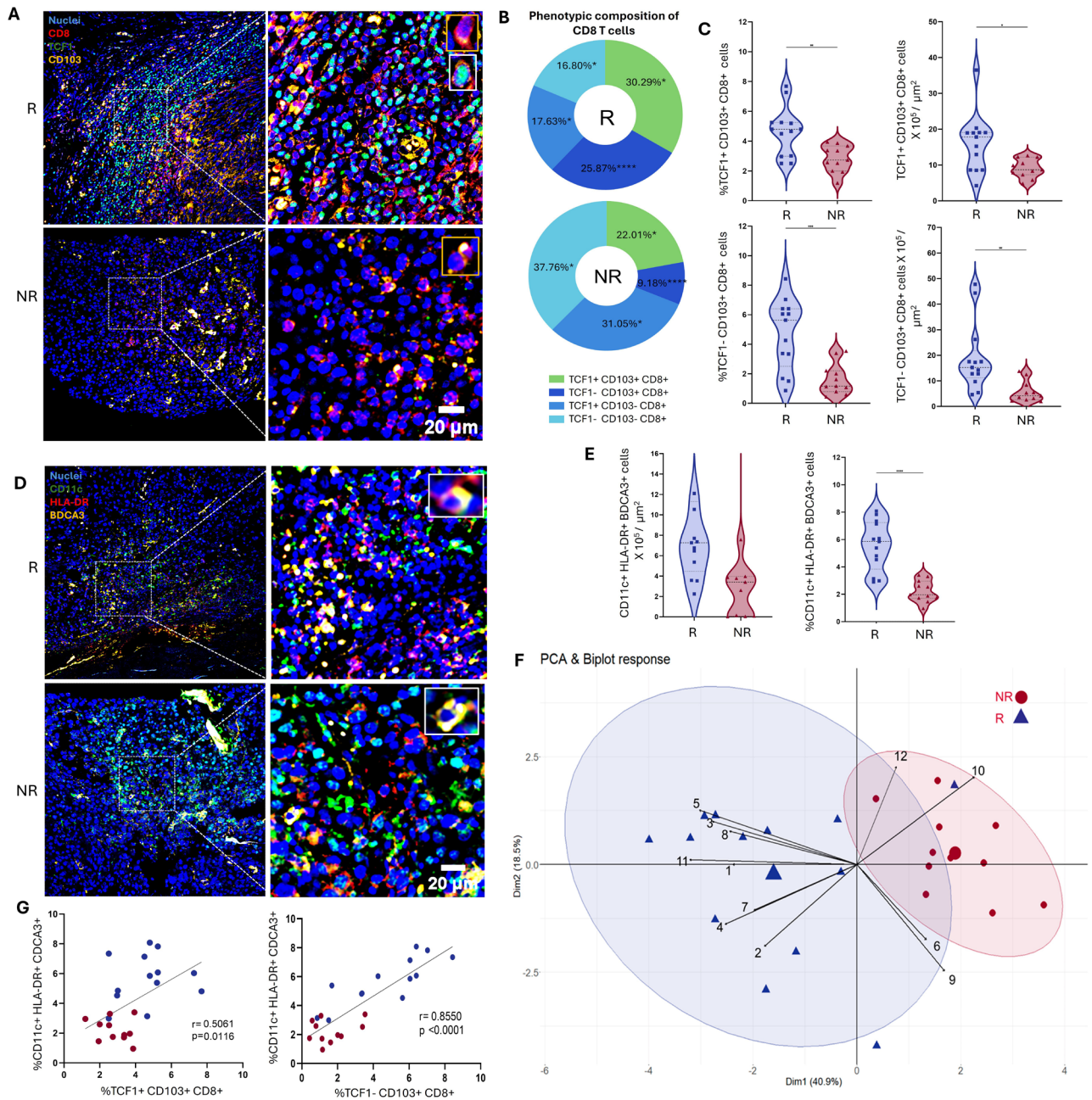


Figure 7 TCF1+ and TCF1- TRM CD8 T cells and cDC1s associate with CBI response. (A) Immunofluorescence (IF) staining for CD8 (red), CD103 (yellow), TCF1 (green), and nuclei (blue) in a cohort of patients treated with checkpoint blockade immunotherapy (CBI). White squares illustrate an example of TCF1+ and yellow squares TCF1- cells. (B) Pie charts depicting the proportion of TCF1, CD103, and CD8 positivity with respect to the fraction of CD8+ cells in patients divided as responders (R) or non-responders (NR). (C) Quantifications of percentage (left) and tissue density per area (right) of TCF1+CD103+ CD8 T cells (top) and TCF1- CD103+CD8 T cells (bottom). (D) IF staining for CD11c (green), HLA-DR (red), BDCA3 (yellow) and nuclei (blue), white square illustrating the positivity of the three marks. (E) Quantifications of percentage (top) and density (bottom) of CD11c+HLA-DR+ BDCA3+ cell populations. (F) PCA plot, each blue dot represents an R patient (n=10), and red triangles represent NR patients (n=9). The resulting grouping was obtained by PCA of 12 immune cell population measurements. As a result, each measurement is denoted by black vectors with the corresponding match number from vectors: 1 (%CD8+), 2 (CD8+ tissue density), 3 (%CD103+CD8+), 4 (%TCF1+CD103+ CD8+), 5 (%TCF1- CD103+CD8+), 6 (%TCF1+CD103- CD8+), 7 (%TCF1+CD103+ CD8+ of total CD8+ cells), 8 (%TCF1- CD103+CD8+ of total CD8+ cells), 9 (%TCF1+CD103- CD8+ of total CD8+ cells), 10 (%TCF1- CD103- CD8+ of total CD8+ cells), 11 (%cDC1 cells with respect to the total infiltrate) and 12 (%CD11c with respect to the total infiltrate). (G) Simple linear regression and Spearman's correlation tests between %TCF1+CD103+ CD8+ cells and %cDC1s (left) and between %TCF1- CD103+CD8+ cells and %cDC1s (right). Unpaired t-test, *p<0.05, **p<0.01, ***p<0.001 and ****p<0.0001.

with cDC1 expansion via FLT3 ligands exhibit enhanced protection against melanoma rechallenge.^{34 67} There is emerging evidence of cDC1's responsiveness to CBI in murine cancer models.^{34 35 68} However, to the best of our knowledge, this is the first evidence supporting the capacity of cDC1 to respond to CBI in a clinical setting. A recent murine study suggests that highly immunogenic tumors do not require TCF1 expression to respond to CBI, indicating that responses of cutaneous melanoma are independent of TCF1.⁶⁹ We observed that cutaneous melanoma relies on TCF1 expression for both tumor control and CBI response. Furthermore, multiple lines of evidence support the importance of *TCF7*/*TCF1* expression in melanoma, as demonstrated in experimental animal models^{6 70} and clinical studies.^{4 22 71}

Transcriptional studies underscore the importance of *TCF7*-expressing CD8 T cell in anti-PD1 and anti-CTLA4 CBI responses.^{5 6 20–23} However, previous studies support a mutual exclusivity between the expression of the tissue residency program and *TCF7*.^{24–27} Our data unequivocally demonstrate the existence of TCF1+TRMCD8 T cells, validating their crucial role in melanoma control and CBI response. Similar *TCF7*+/*TCF1*+TRMCD8 T cells have been observed in murine models of infection and human cancer, and we have documented their presence in murine melanoma, adding to their relevance in immunosurveillance.^{28–32}

It is plausible that the above-mentioned studies may have predominantly focused on the highly cytolytic TRM subset expressing high levels of *PRDM1*, *HOBIT* and *BCL11b* transcription factors.^{25–27 29} This subset likely resides within the TCF1– TRM, suggesting a potential misinterpretation of previous data. Notably, the group led by AW Goldrath has observed two distinct TRM stages, a progenitor TRM dependent on transcription factor ID3, and an exhausted TRM dependent on BLIMP1.^{18 31} The former is characterized by expression of *TCF7* while the latter exhibits coexpression of cytolytic and exhaustion markers. These TRM stages align well with our identified TCF1+ and TCF1– TRM stages. Alternatively, *TCF7* expression without *ITGAE* (encoding CD103) might have been observed in T cells differentiating to the central memory compartment, which were erroneously assigned to TRM.

TCF1 serves as a marker of stemness features, for instance, in murine embryonic stem cells TCF1 drives self-renewal.⁷² TCF1 is also important for early thymic T cell differentiation and late peripheral maturation.⁷³ Better exemplified in chronic infections, TCF1 expression is critical for maintaining effector memory T cells, as evidenced by *TCF7* knockout mice failing to respond to secondary challenges.^{74 75} *TCF7* expression also characterizes progenitor PD1+ memory T cells that expand on CBI treatment, giving rise to more effector and exhausted populations.^{6 17 21} Our data are consistent with a scenario where TCF1+ TRMCD8 T cells give rise to TCF1– cells with enhanced cytotoxic capacity. Both TRM subsets seem to effectively control tumor growth and are enriched in

CBI-responding patients. Accumulation of checkpoint inhibitors, especially in the most cytolytic TCF1– subset, hints patients losing melanoma control. A transcriptional and chromatin structure study also supports this differentiation trajectory, where stem TRM T cells progressively differentiates into effector/pre-exhausted to truly exhausted cells.²⁸

CD103– CD8 T cells were consistently associated with a poor prognosis in both CBI-naïve and CBI-treated cohorts and the TCGA melanoma database. Given that close to 90% of CD103+ CD8T cells express other residency markers, these cells likely are not TRM. Although the CD103– population was not further explored, TCF1+ cells within this subset may represent bystander naïve or recently primed T cells. Even if they belong to other memory CD8 T cells, the superior effector activity of TRM CD8 has been previously demonstrated, particularly in T cells challenged by chronic antigens and expressing checkpoint inhibitors.^{8–10} Noteworthy, our data underscore the utility of staining with a panel of seven markers (TCF1, CD103, CD8, BDCA3, CD11c, HLA-DR and nuclei) to identify patients with enhanced risk of unfavorable outcome and patients who would benefit from CBI, a staining protocol readily achievable in hospitals from developing countries. While many studies attempt to use a single cell type or a single marker as a predictor of prognosis or response to CBI, we propose evaluating at least three different immune populations working together in response to the tumor.

In summary, our study presents a compelling narrative wherein TCF1+ TRMCD8 T cells and cDC1 cells play a central role in mediating melanoma control. These populations are also pivotal to the therapeutic benefits of CBI. This assertion is based on the capacity of cDC1s to cross-activate CD8 T cells, including TRMs, and the ability of TCF1+ CD8 TRMs to maintain a progenitor population that gives rise to TCF1– CD8 TRMs with heightened effector function, despite the expression of checkpoint inhibitors.

Study limitations

This study has several limitations that warrant consideration. First, the cohort exhibits significant heterogeneity in treatment regimens, reflecting the diverse clinical practices and access to immunotherapeutic agents across multiple oncology centers. This heterogeneity may introduce variability in treatment responses and outcomes, potentially impacting the generalizability of our findings. Second, the number of patients in our cohort who received CBI is small, comprising only 24 individuals. Future studies should aim to include larger cohorts of patients and extended follow-up periods, particularly for patients with acral melanoma, to validate whether the importance we observed for the TCF1+ and TCF1– CD8 TRMs and cDC1 populations in this specific melanoma subtype, also translates into CBI response. Despite these limitations, our study provides valuable insights

into TCF1+ and TCF1- CD8 TRMs and cDC1s, laying the groundwork for future research in this area.

Author affiliations

¹Posgrado en Ciencias Biológicas, Facultad de Medicina, Universidad Nacional Autónoma de México, Mexico City, Mexico

²Unidad de Investigación Médica en Inmunoquímica, UMAE Hospital de Especialidades, Centro Médico Nacional Siglo XXI, Instituto Mexicano del Seguro Social, Ciudad de Mexico, Mexico

³Unidad de Investigación Médica en Inmunología, UMAE Hospital de Pediatría, Centro Médico Nacional Siglo XXI, Instituto Mexicano del Seguro Social, Ciudad de Mexico, Mexico

⁴Posgrado en Ciencias Bioquímicas, Facultad de Química, Universidad Nacional Autónoma de México, Mexico City, Mexico

⁵Unidad de Investigación en Virología y Cáncer, Hospital Infantil de Mexico Federico Gomez, Mexico City, Mexico

⁶Servicio de Patología, Hospital de Oncología Centro Médico Nacional Siglo XXI, Instituto Mexicano del Seguro Social, Ciudad de Mexico, Mexico

⁷Medical Center American British Cowdray, Mexico City, Mexico

⁸Latin American Network for Cancer Research (LAN-CANCER), Lima, Peru

⁹UMAE Hospital de Especialidades, Centro Médico Nacional General Manuel Avila Camacho, Instituto Mexicano del Seguro Social, Puebla, Mexico

¹⁰Unidad Médica de Alta Especialidad No.25, Instituto Mexicano del Seguro Social, Monterrey, Nuevo Leon, Mexico

¹¹División de Atención Oncológica en Adultos. Coordinación de Atención Oncológica, Instituto Mexicano del Seguro Social, Ciudad de Mexico, Mexico

¹²Coordinación de investigación en salud, Centro Médico Nacional Siglo XXI, Instituto Mexicano del Seguro Social, Ciudad de Mexico, Mexico

X Sarai G De León-Rodríguez @deleonr_g and Ezequiel M Fuentes-Panana @FuentesPanana

Acknowledgements This paper serves as a fulfillment of SGDL-R to obtain a Doctoral degree in the Programa de Doctorado en Ciencias Biológicas, UNAM in Biomedicine field of knowledge. SGDL-R acknowledges to Programa de Doctorado, Postgrado en Ciencias Biológicas, Universidad Nacional Autónoma de México (UNAM) and Consejo Nacional de Ciencia Tecnología (CONAHCyT) fellowship 1084890. The authors acknowledge the help of PhD. Samira Muñoz for the kind feedback she provided throughout the writing process. We deeply acknowledge Dr. Alma Segura from UMAA199 for providing us with two patients to enhance our ICB cohort. We thank PhD. Vadim Perez Koldenkova for his technical support in confocal microscopy at Laboratorio Nacional de Microscopia Avanzada from Coordinación en Salud at Centro Médico Nacional Siglo XXI IMSS. We also thank histotechnologist Adrian Palma and Victor Torres for performing the histological tissue sections. JAG acknowledges to Programa de Doctorado en Ciencias Bioquímicas, Universidad Nacional Autónoma de México (UNAM) and Consejo Nacional de Ciencia y Tecnología (CONAHCyT) fellowship 832712. AJF acknowledges CONAHCyT-PRONACES 302962 for the postdoctoral fellowship received (775924). We also acknowledge ChapGPT 3.5 for helping us to review grammar and writing style. We also acknowledge the support of The Dirección de Investigación, of Hospital Infantil de México “Federico Gómez”.

Contributors Guarantors of the study are LCB and EMF-P; Generation of cohorts A and B: AM, RG-C, JFM-H, DAV-O, CTG-Q, SB-C, MAS-P, EC-M, and SRR; Data curation, acquisition, analysis, and interpretation of data: SGDL-R, CA-F, JAG, AJ-F, LCB, and EMF-P; Statistical analysis: SGDL-R, JAG and AJ-F; Drafting of the manuscript: SGDL-R, JAG, CA-F, LCB and EMF-P; Critical revision of the manuscript for important intellectual content: AM, RG-C, JFM-H, DAV-O, CTG-Q, SB-C, MAS-P, EC-M, and SRR; Obtained funding: LCB; Study supervision: EMF-P and LCB; Visualization, LCB and EMF-P.

Funding This study was funded by CONAHCyT-PRONACES 302962.

Competing interests None declared.

Patient consent for publication Consent obtained directly from patient(s).

Ethics approval This study involves human participants and the study received approval from the Scientific, Ethical, and Biosafety committees of participating hospitals: Instituto Mexicano del Seguro Social (IMSS) (R-2020-785-04), and Centro Médico ABC (ABC-21-39). Participants gave informed consent to participate in the study before taking part.

Provenance and peer review Not commissioned; externally peer reviewed.

Data availability statement All data relevant to the study are included in the article or uploaded as online supplemental information.

Supplemental material This content has been supplied by the author(s). It has not been vetted by BMJ Publishing Group Limited (BMJ) and may not have been peer-reviewed. Any opinions or recommendations discussed are solely those of the author(s) and are not endorsed by BMJ. BMJ disclaims all liability and responsibility arising from any reliance placed on the content. Where the content includes any translated material, BMJ does not warrant the accuracy and reliability of the translations (including but not limited to local regulations, clinical guidelines, terminology, drug names and drug dosages), and is not responsible for any error and/or omissions arising from translation and adaptation or otherwise.

Open access This is an open access article distributed in accordance with the Creative Commons Attribution Non Commercial (CC BY-NC 4.0) license, which permits others to distribute, remix, adapt, build upon this work non-commercially, and license their derivative works on different terms, provided the original work is properly cited, appropriate credit is given, any changes made indicated, and the use is non-commercial. See <http://creativecommons.org/licenses/by-nc/4.0/>.

ORCID iDs

Sarai G De León-Rodríguez <http://orcid.org/0000-0002-2451-0123>

Ezequiel M Fuentes-Panana <http://orcid.org/0000-0003-2872-0459>

Laura C Bonifaz <http://orcid.org/0000-0001-8482-5648>

REFERENCES

- 1 Wolchok JD, Chiarion-Sileni V, Gonzalez R, *et al.* Long-term outcomes with Nivolumab plus Ipilimumab or Nivolumab alone versus Ipilimumab in patients with advanced Melanoma. *J Clin Oncol* 2022;40:127–37.
- 2 Blank CU, Haining WN, Held W, *et al.* Defining 'T cell exhaustion'. *Nat Rev Immunol* 2019;19:665–74.
- 3 Speiser DE, Utzschneider DT, Oberle SG, *et al.* T cell differentiation in chronic infection and cancer: functional adaptation or exhaustion? *Nat Rev Immunol* 2014;14:768–74.
- 4 Miller BC, Sen DR, Al Abosy R, *et al.* Subsets of exhausted CD8+ T cells differentially mediate tumor control and respond to checkpoint blockade. *Nat Immunol* 2019;20:326–36.
- 5 Beltra J-C, Manne S, Abdel-Hakeem MS, *et al.* Developmental relationships of four exhausted CD8+ T cell subsets reveals underlying transcriptional and epigenetic landscape control mechanisms. *Immunity* 2020;52:825–41.
- 6 Siddiqui I, Schaeuble K, Chennupati V, *et al.* Intratumoral TCF1+PD-1+CD8+ T cells with stem-like properties promote tumor control in response to vaccination and checkpoint blockade immunotherapy. *Immunity* 2019;50:195–211.
- 7 Yu YR, Imrichova H, Wang H, *et al.* Disturbed mitochondrial dynamics in CD8+ TILs reinforce T cell exhaustion. *Nat Immunol* 2020;21:1540–51.
- 8 Ganesan AP, Clarke J, Wood O, *et al.* Tissue-resident memory features are linked to the magnitude of cytotoxic T cell responses in human lung cancer. *Nat Immunol* 2017;18:940–50.
- 9 Pallett LJ, Davies J, Colbeck EJ, *et al.* IL-2High tissue-resident T cells in the human liver: sentinels for hepatotropic infection. *J Exp Med* 2017;214:1567–80.
- 10 Pizzolla A, Keam SP, Vergara IA, *et al.* Tissue-resident memory T cells from a metastatic vaginal Melanoma patient are tumor-responsive T cells and increase after anti-PD-1 treatment. *J Immunother Cancer* 2022;10:e004574.
- 11 Malik BT, Byrne KT, Vella JL, *et al.* Resident memory T cells in the skin mediate durable immunity to Melanoma. *Sci Immunol* 2017;2:eaam6346.
- 12 Edwards J, Wilmott JS, Madore J, *et al.* CD103+ tumor-resident CD8+ T cells are associated with improved survival in Immunotherapy-Naïve Melanoma patients and expand significantly during anti-PD-1 treatment. *Clinical Cancer Research* 2018;24:3036–45.
- 13 Park SL, Buzzai A, Rautela J, *et al.* Tissue-resident memory CD8+ T cells promote Melanoma-immune equilibrium in skin. *Nature* 2019;565:366–71.
- 14 Djenidi F, Adam J, Goubar A, *et al.* CD8+CD103+ tumor-infiltrating lymphocytes are tumor-specific tissue-resident memory T cells and a prognostic factor for survival in lung cancer patients. *J Immunol* 2015;194:3475–86.
- 15 Hartana CA, Ahlén Bergman E, Broomé A, *et al.* Tissue-resident memory T cells are epigenetically cytotoxic with signs of exhaustion in human urinary bladder cancer. *Clin Exp Immunol* 2018;194:39–53.

- 16 Han J, Zhao Y, Shirai K, et al. Resident and circulating memory T cells persist for years in melanoma patients with durable responses to immunotherapy. *Nat Cancer* 2021;2:300–11.
- 17 Chen Z, Ji Z, Ngiow SF, et al. TCF-1-centered transcriptional network drives an effector versus exhausted CD8 T cell-fate decision. *Immunity* 2019;51:840–55.
- 18 Kurd NS, He Z, Louis TL, et al. Early precursors and molecular determinants of tissue-resident memory CD8+ T lymphocytes revealed by single-cell RNA sequencing. *Sci Immunol* 2020;5:eaaz6894.
- 19 Milner JD. Primary Atopic disorders. *Annu Rev Immunol* 2020;38:785–808.
- 20 Im SJ, Hashimoto M, Gerner MY, et al. Defining CD8+ T cells that provide the proliferative burst after PD-1 therapy. *Nature* 2016;537:417–21.
- 21 Jadhav RR, Im SJ, Hu B, et al. Epigenetic signature of PD-1+ TCF1+ CD8 T cells that act as resource cells during chronic viral infection and respond to PD-1 blockade. *Proc Natl Acad Sci U S A* 2019;116:14113–8.
- 22 Sade-Feldman M, Yizhak K, Bjorgaard SL, et al. Defining T cell states associated with response to checkpoint immunotherapy in melanoma. *Cell* 2018;175:998–1013.
- 23 Utzschneider DT, Charmoy M, Chennupati V, et al. T cell factor 1-expressing memory-like CD8(+) T cells sustain the immune response to chronic viral infections. *Immunity* 2016;45:415–27.
- 24 Corgnac S, Malenica I, Mezquita L, et al. CD103+CD8+ TRM cells accumulate in tumors of anti-PD-1-responder lung cancer patients and are tumor-reactive lymphocytes enriched with TC17. *Cell Reports Medicine* 2020;1:100127.
- 25 Mackay LK, Minnich M, Kragten NAM, et al. Hobit and Blimp1 instruct a universal transcriptional program of tissue residency in lymphocytes. *Science* 2016;352:459–63.
- 26 Davé VA, Cardozo-Ojeda EF, Mair F, et al. Cervicovaginal tissue residence confers a distinct differentiation program upon memory CD8 T cells. *J Immunol* 2021;206:2937–48.
- 27 Wu J, Madi A, Mieg A, et al. T cell factor 1 suppresses CD103+ lung tissue-resident memory T cell development. *Cell Rep* 2020;31:107484.
- 28 Anadón CM, Yu X, Hånggi K, et al. Ovarian cancer immunogenicity is governed by a narrow subset of progenitor tissue-resident memory T cells. *Cancer Cell* 2022;40:545–57.
- 29 Helm EY, Zelenka T, Cismasiu VB, et al. BCL11B sustains multipotency and restricts effector programs of intestinal-resident memory CD8+ T cells. *Sci Immunol* 2023;8:MC10231135.
- 30 León-Letelier RA, Castro-Medina DI, Badillo-Godinez O, et al. Induction of progenitor exhausted tissue-resident memory CD8+ T cells upon salmonella Typhi Porins adjuvant immunization correlates with melanoma control and anti-PD-1 immunotherapy cooperation. *Front Immunol* 2020;11:583382.
- 31 Milner JJ, Toma C, He Z, et al. Heterogenous populations of tissue-resident CD8+ T cells are generated in response to infection and malignancy. *Immunity* 2020;52:808–24.
- 32 Robinson MH, Vasquez J, Kaushal A, et al. Subtype and grade-dependent spatial heterogeneity of T-cell infiltration in pediatric glioma. *J Immunother Cancer* 2020;8:e001066.
- 33 den Haan JMM, Lehar SM, Bevan MJ. CD8(+) but not CD8(-) Dendritic cells cross-prime cytotoxic T cells in vivo. *J Exp Med* 2000;192:1685–96.
- 34 Sánchez-Paulete AR, Cueto FJ, Martínez-López M, et al. Cancer immunotherapy with immunomodulatory anti-CD137 and anti-PD-1 monoclonal antibodies requires BATF3-dependent Dendritic cells. *Cancer Discovery* 2016;6:71–9.
- 35 Salmon H, Idoyaga J, Rahman A, et al. Expansion and activation of CD103+ Dendritic cell progenitors at the tumor site enhances tumor responses to therapeutic PD-L1 and BRAF inhibition. *Immunity* 2016;44:924–38.
- 36 De León Rodríguez SG, Hernández Herrera P, Aguilar Flores C, et al. A machine learning Workflow of multiplexed Immunofluorescence images to Interrogate activator and Tolerogenic profiles of conventional type 1 dendritic cells infiltrating Melanomas of disease-free and metastatic patients. *J Oncol* 2022;2022:9775736.
- 37 De León-Rodríguez SG, Aguilar-Flores C, Gajón JA, et al. Acral Melanoma is infiltrated with cDC1s and functional exhausted CD8 T cells similar to the cutaneous Melanoma of sun-exposed skin. *Int J Mol Sci* 2023;24:4786.
- 38 Ghislat G, Cheema AS, Baudoin E, et al. NF-κB-dependent IRF1 activation programs cDC1 Dendritic cells to drive antitumor immunity. *Sci Immunol* 2021;6:34244313.
- 39 Stoltzfus CR, Filipek J, Gern BH, et al. Cytomap: a spatial analysis toolbox reveals features of myeloid cell organization in lymphoid tissues. *Cell Rep* 2020;31:107523.
- 40 Cheuk S, Schlums H, Gallais Sérézal I, et al. CD49A expression defines tissue-resident CD8+ T cells poised for cytotoxic function in human skin. *Immunity* 2017;46:287–300.
- 41 Clarke J, Panwar B, Madrigal A, et al. Single-cell transcriptomic analysis of tissue-resident memory T cells in human lung cancer. *J Exp Med* 2019;216:2128–49.
- 42 Hombrink P, Helbig C, Backer RA, et al. Programs for the persistence, vigilance and control of human CD8+ lung-resident memory T cells. *Nat Immunol* 2016;17:1467–78.
- 43 Ida S, Takahashi H, Kawabata-Iwakawa R, et al. Tissue-resident memory T cells correlate with the inflammatory tumor microenvironment and improved prognosis in head and neck squamous cell carcinoma. *Oral Oncol* 2021;122:105508.
- 44 Olalekan S, Xie B, Back R, et al. Characterizing the tumor microenvironment of metastatic ovarian cancer by single-cell transcriptomics. *Cell Rep* 2021;35:109165.
- 45 Peng T, Phasouk K, Bossard E, et al. Distinct populations of antigen-specific tissue-resident CD8+ T cells in human cervix mucosa. *JCI Insight* 2021;6:e149950.
- 46 Savas P, Virassamy B, Ye C, et al. Single-cell profiling of breast cancer T cells reveals a tissue-resident memory subset associated with improved prognosis. *Nat Med* 2018;24:986–93.
- 47 Xu J, Fang Y, Chen K, et al. Single-cell RNA sequencing reveals the tissue architecture in human high-grade Serous ovarian cancer. *Clinical Cancer Research* 2022;28:3590–602.
- 48 Kumar BV, Ma W, Miron M, et al. Human tissue-resident memory T cells are defined by core transcriptional and functional signatures in Lymphoid and Mucosal sites. *Cell Rep* 2017;20:2921–34.
- 49 Kurihara K, Fujiyama T, Phadungsaksawasdi P, et al. Significance of IL-17A-producing CD8+CD103+ skin resident memory T cells in psoriasis lesion and their possible relationship to clinical course. *J Dermatol Sci* 2019;95:21–7.
- 50 Miron M, Kumar BV, Meng W, et al. Human lymph nodes maintain TCF-1Hi memory T cells with high functional potential and Clonal diversity throughout life. *J Immunol* 2018;201:2132–40.
- 51 Schreiner D, King CG. CD4+ memory T cells at home in the tissue: mechanisms for health and disease. *Front Immunol* 2018;9:2394.
- 52 Szabo PA, Miron M, Farber DL. Location, location, location: tissue resident memory T cells in mice and humans. *Sci Immunol* 2019;4:eaas9673.
- 53 Lee AH, Sun L, Mochizuki AY, et al. Neoadjuvant PD-1 blockade induces T cell and cDC1 activation but fails to overcome the immunosuppressive tumor associated Macrophages in recurrent glioblastoma. *Nat Commun* 2021;12:6938.
- 54 Li C, Hua K. Dissecting the single-cell transcriptome network of immune environment underlying cervical premalignant lesion, cervical cancer and metastatic lymph nodes. *Front Immunol* 2022;13:MC9263187.
- 55 Ma W, Lee J, Backenroth D, et al. Single cell RNA-Seq reveals pre-cDCs fate determined by transcription factor combinatorial dose. *BMC Mol Cell Biol* 2019;20:20.
- 56 Villani A-C, Satija R, Reynolds G, et al. Single-cell RNA-Seq reveals new types of human blood Dendritic cells, monocytes, and progenitors. *Science* 2017;356:eaah4573.
- 57 Balan S, Arnold-Schrauf C, Abbas A, et al. Large-scale human Dendritic cell differentiation revealing notch-dependent lineage Bifurcation and heterogeneity. *Cell Rep* 2018;24:1902–15.
- 58 Heger L, Hatscher L, Liang C, et al. XCR1 expression distinguishes human conventional Dendritic cell type 1 with full effector functions from their immature precursors. *Proc Natl Acad Sci U S A* 2023;120:e2300343120.
- 59 Cheng S, Li Z, Gao R, et al. A Pan-cancer single-cell transcriptional Atlas of tumor infiltrating myeloid cells. *Cell* 2021;184:792–809.
- 60 Hänzelmann S, Castelo R, Guinney J. GSEA: gene set variation analysis for microarray and RNA-Seq data. *BMC Bioinformatics* 2013;14:7.
- 61 Langfelder P, Horvath S. WGCNA: an R package for weighted correlation network analysis. *BMC Bioinformatics* 2008;9:559.
- 62 Keung EZ, Gershenwald JE. The eighth edition American joint committee on cancer (AJCC) Melanoma staging system: implications for Melanoma treatment and care. *Expert Rev Anticancer Ther* 2018;18:775–84.
- 63 Hoffmann JC, Schön MP. Integrin AE(Cd103)B7 in epithelial cancer. *Cancers* 2021;13:MC8699740.
- 64 Sullivan RJ, Atkins MB, Kirkwood JM, et al. An update on the society for immunotherapy of cancer consensus statement on tumor immunotherapy for the treatment of cutaneous Melanoma: version 2.0. *J Immunother Cancer* 2018;6:44.
- 65 Gajón JA, Juárez-Flores A, De León Rodríguez SG, et al. Immunotherapy options for Acral Melanoma, A fast-growing but neglected malignancy. *Arch Med Res* 2022;53:794–806.

- 66 Meiser P, Knolle MA, Hirschberger A, *et al.* A distinct stimulatory cDC1 subpopulation Amplifies CD8+ T cell responses in tumors for protective anti-cancer immunity. *Cancer Cell* 2023;41:1498–515.
- 67 Lin DS, Tian L, Tomei S, *et al.* Single-cell analyses reveal the Clonal and molecular Aetiology of Flt3L-induced emergency Dendritic cell development. *Nat Cell Biol* 2021;23:219–31.
- 68 Gilardi M, Saddawi-Konefka R, Wu VH, *et al.* Microneedle-mediated intratumoral delivery of anti-CTLA-4 promotes cDC1-dependent eradication of oral squamous cell carcinoma with limited irAEs. *Molecular Cancer Therapeutics* 2022;21:616–24.
- 69 Escobar G, Tooley K, Oliveras JP, *et al.* Tumor immunogenicity dictates reliance on TCF1 in CD8+ T cells for response to immunotherapy. *Cancer Cell* 2023;41:1662–79.
- 70 Shan Q, Hu S, Chen X, *et al.* Ectopic TCF1 expression Instills a stem-like program in exhausted CD8+ T cells to enhance viral and tumor immunity. *Cell Mol Immunol* 2021;18:1262–77.
- 71 Oba T, Long MD, Ito KI, *et al.* Clinical and immunological relevance of SLAMF6 expression in the tumor microenvironment of breast cancer and Melanoma. *Sci Rep* 2024;14:2394.
- 72 De Jaime-Soguero A, Aulicino F, Ertaylan G, *et al.* WNT/TCF1 pathway restricts embryonic stem cell cycle through activation of the Ink4/ARF locus. *PLoS Genet* 2017;13:e1006682.
- 73 Yu Q, Sharma A, Sen JM. TCF1 and beta-Catenin regulate T cell development and function. *Immunol Res* 2010;47:45–55.
- 74 Jeannet G, Boudousquié C, Gardiol N, *et al.* Essential role of the WNT pathway effector TCF-1 for the establishment of functional CD8 T cell memory. *Proc Natl Acad Sci U S A* 2010;107:9777–82.
- 75 Zhou X, Xue HH. Cutting edge: generation of memory precursors and functional memory CD8+ T cells depends on T cell Factor-1 and Lymphoid enhancer-binding Factor-1. *J Immunol* 2012;189:2722–6.